

**GEOPHYSICAL REPORT FOR WORK COMPLETED ON JULY 16, 2001  
TANNER CLAIMS  
TANNER 1 – 8, YC02343 TO YC02350  
MAYO MINING DISTRICT  
106 C/03  
MOUNT FERRELL/ NADALEEN RIVER AREA  
64°03' W and 133°15'N**

**MANSON CREEK RESOURCES LTD  
SUITE 500, 926 – 5<sup>TH</sup> AVE SW  
CALGARY, AB  
T2P 0N7**

Regan Chernish P.Geol  
Geological Consultant



094298 V.1

Geophysical Report to accompany statement of work filed in August 2001.

This report has been examined by  
the Geological Evaluation Unit  
under Section 53 (4) Yukon Quartz  
Mining Act and is allowed as  
representation work in the amount  
of \$ 9668.16.

*M. B.*  
Regional Manager, Exploration and  
Geological Services for Commissioner  
of Yukon Territory.

**TABLE OF CONTENTS**

**1.0 INTRODUCTION**

**2.0 DESCRIPTION OF LANDHOLDINGS**

**2.1 LOCATION AND MINERAL CLAIMS**

**2.2 ACCESS**

**2.3 PROPERTY HISTORY**

**3.0 GENERAL GEOLOGY**

**3.1a SHALES**

**3.1b CLASTICS AND CARBONATES**

**3.1c INTRUSIONS**

**4.0 STRUCTURE**

**5.0 2001 AIRBORNE GEOPHYSICAL SURVEY**

**5.1 GEOPHYSICAL INSTRUMENTS AND METHODS**

**6.0 AIRBORNE SURVEY RESULTS**

**7.0 CONCLUSIONS AND RECOMMENDATION**

**8.0 REFERENCES**

**9.0 STATEMENT OF COSTS**

**10.0 CERTIFICATION**

**LIST OF MAPS**

**YUKON ENERGY, MINES  
& RESOURCES LIBRARY**  
P.O. Box 2703  
Whitehorse, Yukon Y1A 2C6

## **1.0 INTRODUCTION**

The Tanner claims consist of eight contiguous claims originally staked in the summer of 2000 by Anne Bordeleau. In June 2001, Manson Creek Resources Ltd. ("Manson Creek") entered into an option agreement with Ms. Bordeleau on the Tanner Claims and title was transferred to Manson Creek on June 28, 2001. The claims, Tanner 1 – 8 (YC02343 – YC02350), were prospected in late summer 2000 and Manson Creek decided that a follow up airborne survey would be of use in the understanding and evaluation of the property.

Manson Creek commissioned FUGRO AIRBORNE SURVEYS to fly an airborne geophysical survey over the Tanner Claims. On July 16, 2001, an airborne survey consisting of 57-line km of magnetics, electromagnetics and radiometrics was flown and completed on the Property.

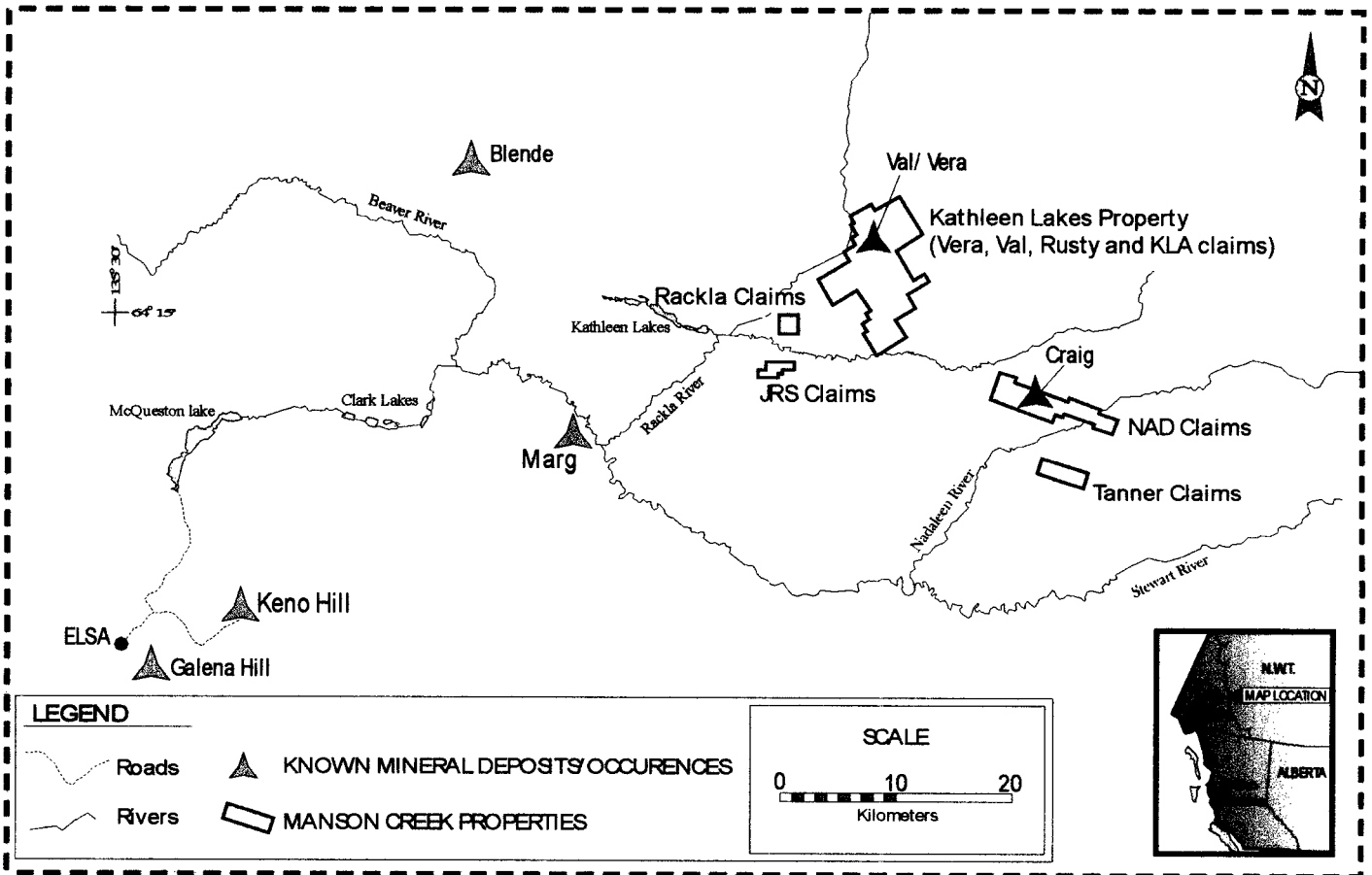
This report is to accompany the statement of work filed in Mayo in August 2001.



## 2.1 LOCATION AND MINERAL CLAIMS

The Tanner Claims are located in the Mayo Mining district (Figure 1), approximately 64°03' N and 133° 15' W, NTS sheet 106C/03. The claims are located approximately 130 km north-northeast of Mayo.

Figure 1. Location of Claims.

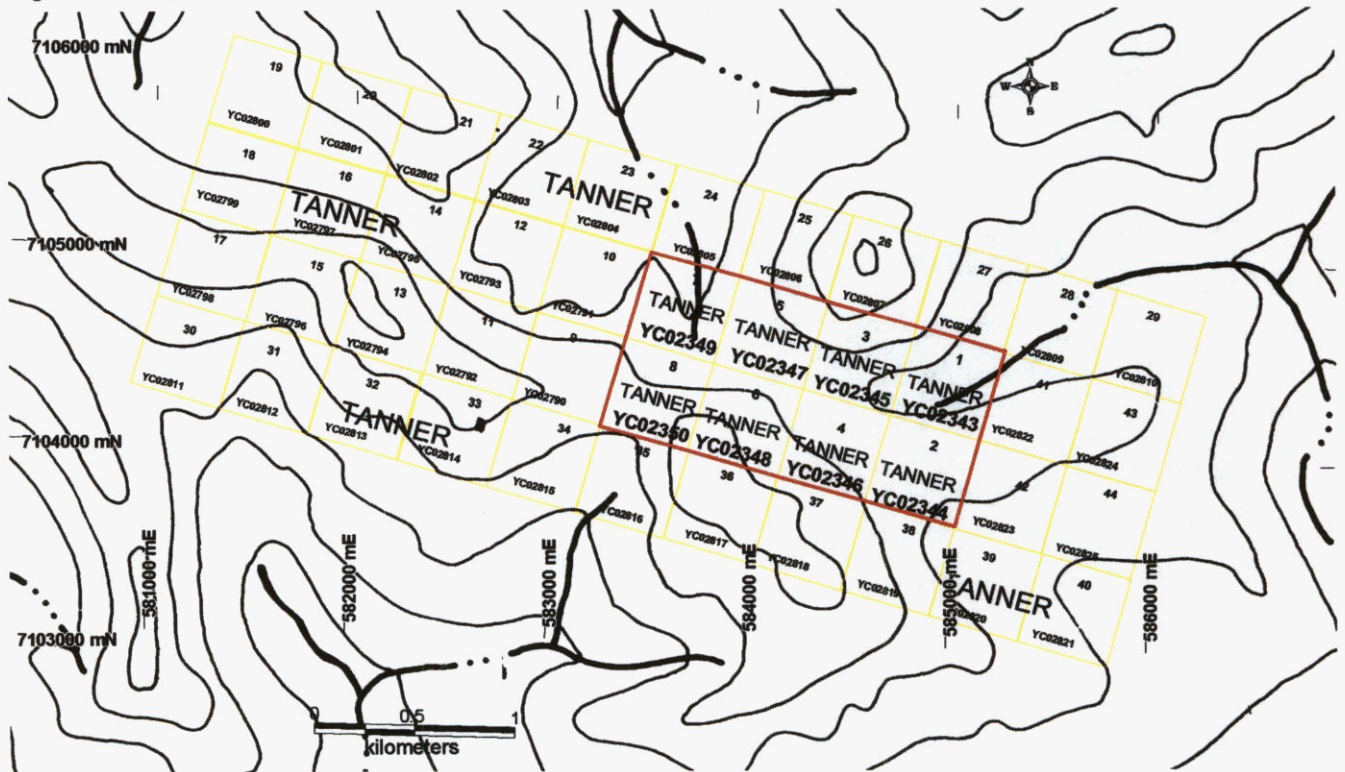


The Tanner block is comprised of eight contiguous claims (Figure 2), the Tanner 1 – 8 claims (YC02343 to YC02350).

List of Claims:

CLAIM NAME	GRANT NUMBER	TITLE HOLDER OF CLAIMS
TANNER 1	YC02343	Manson Creek Resources Ltd
TANNER 2	YC02344	Manson Creek Resources Ltd
TANNER 3	YC02345	Manson Creek Resources Ltd
TANNER 4	YC02346	Manson Creek Resources Ltd
TANNER 5	YC02347	Manson Creek Resources Ltd
TANNER 6	YC02348	Manson Creek Resources Ltd
TANNER 7	YC02349	Manson Creek Resources Ltd
TANNER 8	YC02350	Manson Creek Resources Ltd

Figure 2. Tanner Claims



Tanner 1-8 Highlighted in red.

## 2.2 ACCESS

There is no fixed wing access to the Tanner Claim block. To access the block one can fly the 120km from Mayo to the airstrip located at the Rackla camp and then utilize a helicopter to fly the last 18km to the Tanner Claim block. An alternative route is to use a helicopter to fly directly from Mayo to the Tanner Block, a distance of 120km.

## 2.3 PROPERTY HISTORY

The Tanner claims were staked in the summer of 2000 and at that time a limited soil, rock and water sampling program was initiated. Several gossanous streams were identified and sampled.

Later in the summer of 2000, a limited reconnaissance mapping/prospecting program was completed. No previous work has been done in the area of the Tanner Claim block.

### **3.0 GENERAL GEOLOGY**

Mapping in the area has been limited to geological mapping as part of the GSC regional mapping exercises (1:250,000 scale). Specifically, the only regional work performed on the 106 C map sheets outside of late compilation and reinterpretation work was conducted by Blusson 1978. More work was conducted on the 106D (Nash Creek) map sheet, which is adjacent to the West of the project area. Work by Green and Roddick (1961), Blusson (1978) and more recently, work by Grant Abbot (1990) is available for the Nash Creek map sheet. Recent work of interest was also conducted in 1990 by S.P. Gordey on the Tiny Island map sheet (105M/16), south of the Nash Creek map sheet. Many of Mr. Gordey's observations and new interpretations are considered relevant in a regional sense to the Tanner Claim block.

Historically, the district geology has been widely recognized as being underlain by Upper Proterozoic clastic rocks to the South (Hyland Group) and Devonian to Mississippian shales and carbonates to the North (Eam Group) (Grant Abbot, Current Research, GSC Paper 90-1E, 1990). The two units are represented in the literature as being separated by a zone of south dipping thrust faults collectively termed the Dawson Thrust zone. Along this thrust, a package of rocks composed of slate, quartzite, conglomerates and minor volcanic units, informally known as the 'grit unit' is thrust northwards over the Eam Group carbonates and black clastic units.

The project area to date has historically been recognized primarily as a silver-lead-zinc district, with the majority of mineralization discovered to date occurring in the Hyland Group carbonate, clastic and sedimentary rocks. The best known examples of this type of mineralization include the Val-Vera veins and the Craig mineralization.

The Marg deposit also occurs within the Eam Group some 60 Km east of the Tanner claim block. It is a VMS type deposit reportedly grading 6.092 Mt grading 1.76% Cu, 2.46 %Pb, 4.6% Zn, 62.7 gpt Ag and 1.0 gpt Au (source: Yukon mineral property update, January 2000, Mineral Resource Branch, Yukon Government). Marg is a pyrite dominated series of massive sulphide lenses occurring at a stratigraphic change between black shales and underlying quartz+/-sericite schists interpreted to represent altered felsic volcanic units.

### **3.1 STRATIGRAPHY**

The two main lithological packages present on Tanner include shales and overlying clastic/carbonate units. Intrusions are also observed and described below. The uppermost unit in the area, found overlying the clastic package on the Tanner block, consist of deep basinal shale and chert sequences

The "Dawson Thrust" has not been recognized in any of the mapped areas and inferred conformability between the various sequences mapped on and across the different properties allows for the interpretation that the area represents a basinal sequence with shallow to deep marine facies and significant volcanic components. The presence of the volcanic components as well as geochemical results obtained from various volcanic rock types in the area suggests an intracratonic rift environment and associated basinal sedimentation. Extent of rifting is not known at this time due to the paucity of regional data.

#### **3.1a SHALES**

A sequence of shales consistently overly the volcanic units but varies in apparent thickness from 50 to many 100's of meters. Those shales are highly strained by regional deformation and few primary features can be recognized in them. They are locally graphitic, may contain sericitic bands and locally contain sandy interbeds or minor volcanic components (tuffs, minor flows). In

drill core from past drilling within this unit in the area, it is frequently seen to contain thin rhythmic lamina of pyrite and sulphide bands up to 10 cm in thickness.

Barite has been recognized on the Tanner claims.

Discrete beds of sandstones are occasionally found within the shale package. These 'sandstones' are peculiar in the sense that quartz grains have a homogeneous, clear, occasionally angular to bipyramidal appearance. Minor feldspars are found in the beds and the matrix consists of finer grained silica, clays, chlorite or white mica (muscovite?). Rocks of similar description have been ascribed a volcanic origin by Gordey on the Tiny Island map sheet and may represent 'felsic flows, tuffs or both'. Minor pyrite is often found within these units and they are definitely different in composition from the overlying sandstones of the clastic package described below. It is of interest that these monomineralic sandstones have been found to occur locally throughout the volcanic, shale and clastic packages on the Tanner Claims. This could be a lithological argument supporting continuity between the stratigraphic groups described in the area.

### **3.1b CLASTICS AND CARBONATES**

The clastic and carbonate rocks that occur throughout the area have historically been considered part of the Upper Proterozoic Hyland Group. No opinion is presented here regarding this classification and field relationships will be presented as observed in the field. The observations are interpreted within the larger context of the recent regional field mapping programs conducted by Manson Creek.

The clastic and carbonate package is dominated by relatively coarse sandstones, wackes and conglomerates. In addition, there are limy lutites, pelites and recrystallized limestones. The ratios of sandstone to limy sediments/limestones can vary quite significantly on a km scale basis. There are fine to coarse detrital shales present throughout the sequence. Beds are generally laterally extensive and easily correlateable over large areas (10's of KM). Ripple marks have been observed on both sandstone and limy shale surfaces indicating a shallow depositional environment.

The clastic and carbonate package is present throughout the area with an interpreted thickness of no greater than 250 to 300m.

### **3.1c INTRUSIONS**

Gabbroic intrusions have been observed on the Tanner block. It is similar in aspect to many intrusions observed in the area of Rusty Mountain that lies to the north of the Tanner Claims.

The intrusions have a fine to coarse poikilitic textures and a gabbroic composition (based on whole rock geochemistry). It is a possibility that these intrusions are subvolcanic intrusions. This is proposed in light of the observation of a possible eruption of such an intrusion in the sedimentary sequence (forming mafic tuffs/pepperite) on the Tanner block.

The intrusions have not been seen intruding the clastic/carbonate sequence anywhere in the project area.

## **4.0 STRUCTURE**

Three folding events have been recognized on the Tanner block. Numerous structural observations and the interpretation of local and regional mapping data support the presence of predominantly ductile deformation.

## **D1 (S1)**

This dominant feature is related to the first folding event, which was roughly east-west striking. It is characterized by a vertical to south dipping axial plane and associated locally strongly developed axial planar penetrative schistosity (S1). Although the deformation can appear quite spectacular, it is relatively gentle on a regional scale with amplitudes in the order of 100 to 200 meters. Fold closures are generally tight and local overturning of the folded strata is observed.

The difference in competency of the lithological packages gives rise to various expressions of this folding event. Within the clastic package, essentially no schistosity is developed except within some of the shale interbeds. Actual overall fold geometry had to be mapped through recognition of actual fold closure as well as careful mapping of  $S_0$  features.

The shale package has reacted in an extremely ductile fashion to the folding with primary features being largely obliterated by the penetrative S1 schistosity. Bedding can only be discerned locally based on obvious compositional changes within discrete layers (presence of sericitic schists or cherty beds) or within some of the coarser grained intervals (siltstones or sandstones). In most cases, when bedding and S1 are visible, they tend to be in areas where the two are nearly parallel. It is important to note that S1 directions observed in the shales are consistent with axial planar closures observed in the clastic package. At interpreted closures, strong intersection lineation  $S_0/S_1$  'pencil' tectonites are observed.

## **D2 (S2)**

A second folding event has been recognized by the local refolding of the S1 schistosity as well as by the presence of S1/S2 lineations. The weakly developed S2 schistosity is only readily visible in fine-grained shales. It is rarely visible in either the clastic or the volcanic units.

The D2 event is poorly documented due to the difficulties in interpreting the nature of the various intersection lineations. The second folding event is generally considered coplanar to the D1 event, and it may simply represent a reactivation of the first folding event. The effects of D2 are not considered significant in the regional sense and only in certain instances can it have dramatic effects (D2 folding of a D1 fold closure, two such occurrences noted in the field).

## **D3**

The third deformation event has left a structural imprint on the project area. This third event appears to have been more brittle in nature and represents a gentle folding or 'buckling' of the sequence along widely spaced, generally N-S trending, subvertical axial planes. Amplitude of the folding is unclear but is thought to be in the order of 50 to 150 meters.

This deformation is highlighted by numerous North-South intersection lineations in shales and by brittle fracturing in the clastic units, preferentially in the more competent sandstones in proximity to fold closures. Series of S and Z quartz-filled tension gashes/fractures often highlight the actual fold closures in these resistive units. Quartz infilling of fractures associated with this event usually consists of white bull quartz but well developed crystal growth can be noted in some instances. No mineralization has been found in association with this event.

## **5.0 2001 AIRBORNE GEOPHYSICAL SURVEY**

Manson Creek commissioned FUGRO AIRBORNE SURVEYS to fly an airborne geophysical survey over the Tanner Claims. The survey was conducted from the Rackla camp, located 18km to the north of the Tanner block. The airborne survey of the Tanner claims was completed in one day. On July 16, 2001, an airborne survey consisting of 57-line km of magnetics,

electromagnetics and radiometrics was completed on the Tanner block. The flight lines were oriented north south as to cross the stratigraphy as close to perpendicular as possible.

## **5.1 GEOPHYSICAL INSTRUMENTS AND METHODS**

This information and detail is provided in the accompanying Fugro Geophysical Report and will not be duplicated here.

## **6.0 AIRBORNE SURVEY RESULTS**

The geophysical survey area is characterized by an extremely small magnetic gradient (24nT) and a very strong linear conductor that bisects the Property. The magnetic low is on the order of less than 10nT. The airborne survey outlined a 100 to 400m wide conductive zone striking at 122° across the Tanner claims. This 2 to 170 Ohm-m conductor is coincident with to the very weak linear magnetic low.

A small (5-15 meter wide) zone of shearing has been mapped in an area of the coincident magnetic and conductivity. The shearing is possibly related to axial plane stress as it occurs in the heart of a large D1 fold axis. No significant graphite or sulphides have been observed in the exposed shear but clay alteration is strong. The weak magnetic anomaly could be an expression of this shear.

There is no surface expression of the source of the conductive anomaly.

The strongest individual conductors identified along the linear anomaly by the survey occur near large stream gossans. Graphite is known to occur locally in the shales but the presence of the large gossans and their point sources along a linear trend within the conductive corridor highlights the possibility that non-magnetic sulphides may be present at shallow depths. Locally strongly graphitic cherts to the south of the conductivity anomaly do not produce conductivity anomalies of the scale seen in the 'conductivity corridor'.

## **7.0 CONCLUSIONS AND RECOMMENDATION**

The project area is interpreted to represent a transition between volcanic rocks, basinal shales and shallow water clastic and carbonate sedimentary sequences. Volcanism may be related to an intra-cratonic rifting event on the northern edge of the Selwyn Basin and the age of the event can be inferred to be late Proterozoic to Mississippian.

A known volcanogenic massive sulphide deposit of significance is known to occur within strata similar to those described on the project area. The proximity of this occurrence is considered strong evidence that a cluster of deposits with characteristics similar to the Marg occurrence may be discovered with further exploration in the area. A discrete geophysical target was outlined by the airborne geophysical survey over the Tanner block in 2001.

The Geophysical survey outlined a strong linear conductor that is coincident with a very weak linear magnetic low. There is no definitive surface explanation of the source of these anomalies. The presences of the anomalies coincident with a linear trend of large gossans over a wide area may infer proximity at depth of a favourable stratigraphic change (volcanic to sedimentary), which may contain economic mineralization. The conductivity/magnetic anomaly should be drill tested to determine the source of the geophysical responses and determine if it is also the source of the gossans. Should a syngenetic metal-bearing sulphide horizon be recognized, further drilling, ground geophysical work and mapping should be conducted in the area.

### **8.0 REFERENCES**

**Abbot, J.G., 1990, Preliminary results of the stratigraphy and structure of the Mt. Westman map area, central Yukon; in Current Research, Part E, Geological Survey of Canada paper 90-1E, pp. 15-22.**

**Blusson, S.L., 1978, Regional geological setting of Lead-zinc deposits in the Selwyn Basin, Yukon; in Current Research, Part A, Geological Survey of Canada, paper 78-1A, pp. 77-80.**

**Gordey, S.P., 1990, Geology and Mineral Potential, Tiny Island Lake Map Area, Yukon; in Current Research, Part E, Geological Survey of Canada paper 90-1E, pp. 23-29.**

**Green, L.H. and Roddick, J.A., 1961, Geology, Nash Creek, Yukon Territory; Geological Survey of Canada, Map 1282A, scale 1:250,000 (accompanies GSC Memoir 364 by L.H. Green).**

**Yukon MINFILE, 2001. Exploration and Geological Services Division, Yukon, Indian and Northern Affairs Canada**

**10.0 STATEMENT OF COSTS**

Survey Charges

57 km of flying at a fixed rate of \$134.53.00/line-km  
including mobilization costs \$7668.16

Report Preparation

Printing charges and time \$2000.00

**Total to be applied** **\$9668.16**



**9.0 CERTIFICATION**

I, Regan Chernish, of Calgary, Alberta hereby certify that:

I graduated with B.Sc. Geology from the University of Alberta in 1991.

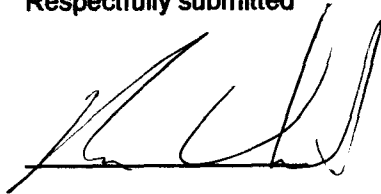
I am a registered Professional Geologist with NAPEGG.

I have been practicing my profession continuously for 10 years.

I am employed as a geological consultant for Manson Creek Resources Ltd.

I was directly involved in the work reported in this document and the associated costs incurred.

Respectfully submitted



Regan Chernish P.Geol

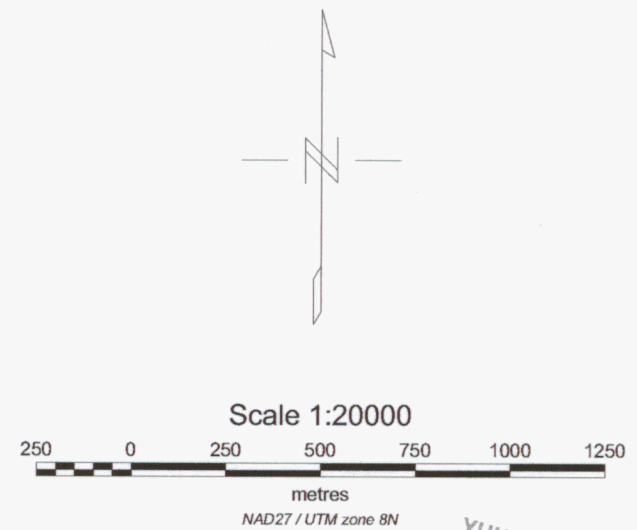
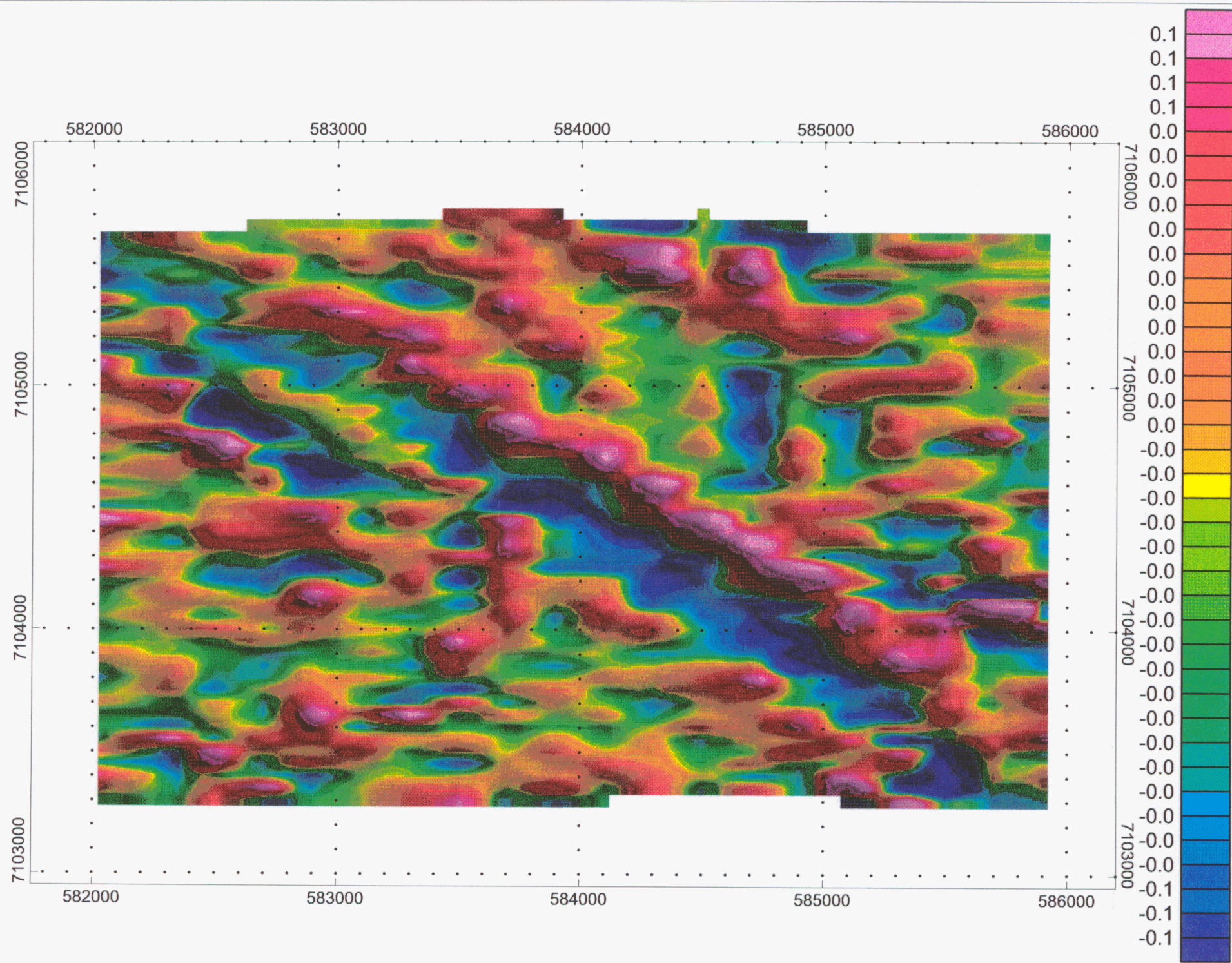


## LIST OF MAPS

1. Total field magnetic
2. Calculated vertical gradient
3. Resistivity 900Hz
4. Resistivity 7200Hz
5. Total count
6. Potassium count
7. Thorium count
8. Uranium count
9. Flight path

YUKON ENERGY, MINES  
& GEOPHYSICS LIBRARY  
PO BOX 100  
Whitehorse, Yukon Y1A 2C8

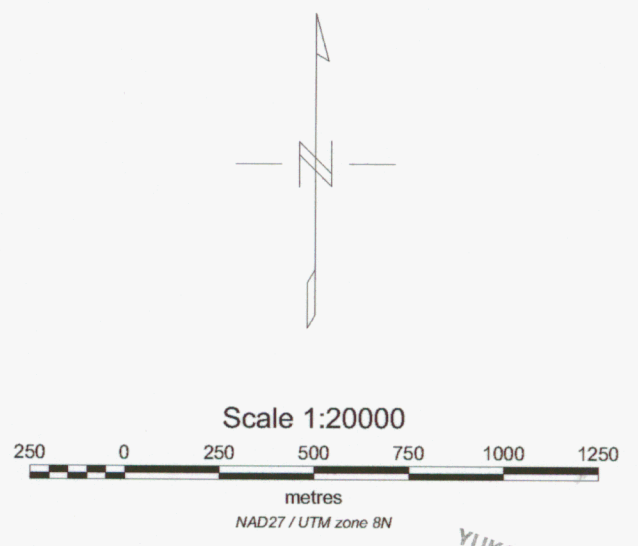
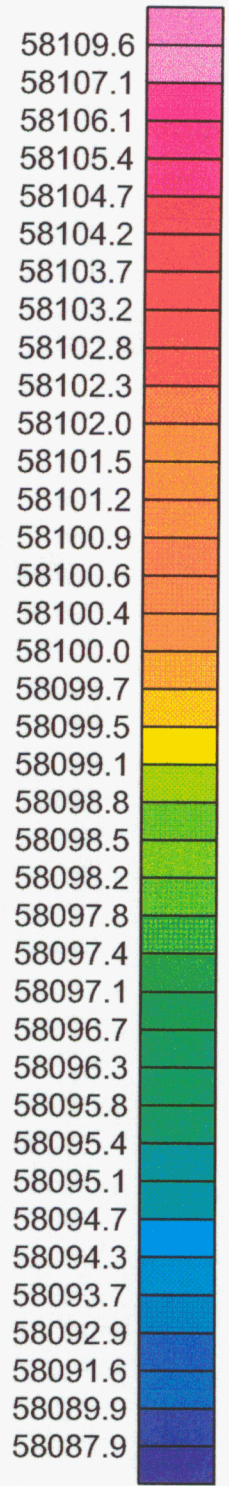
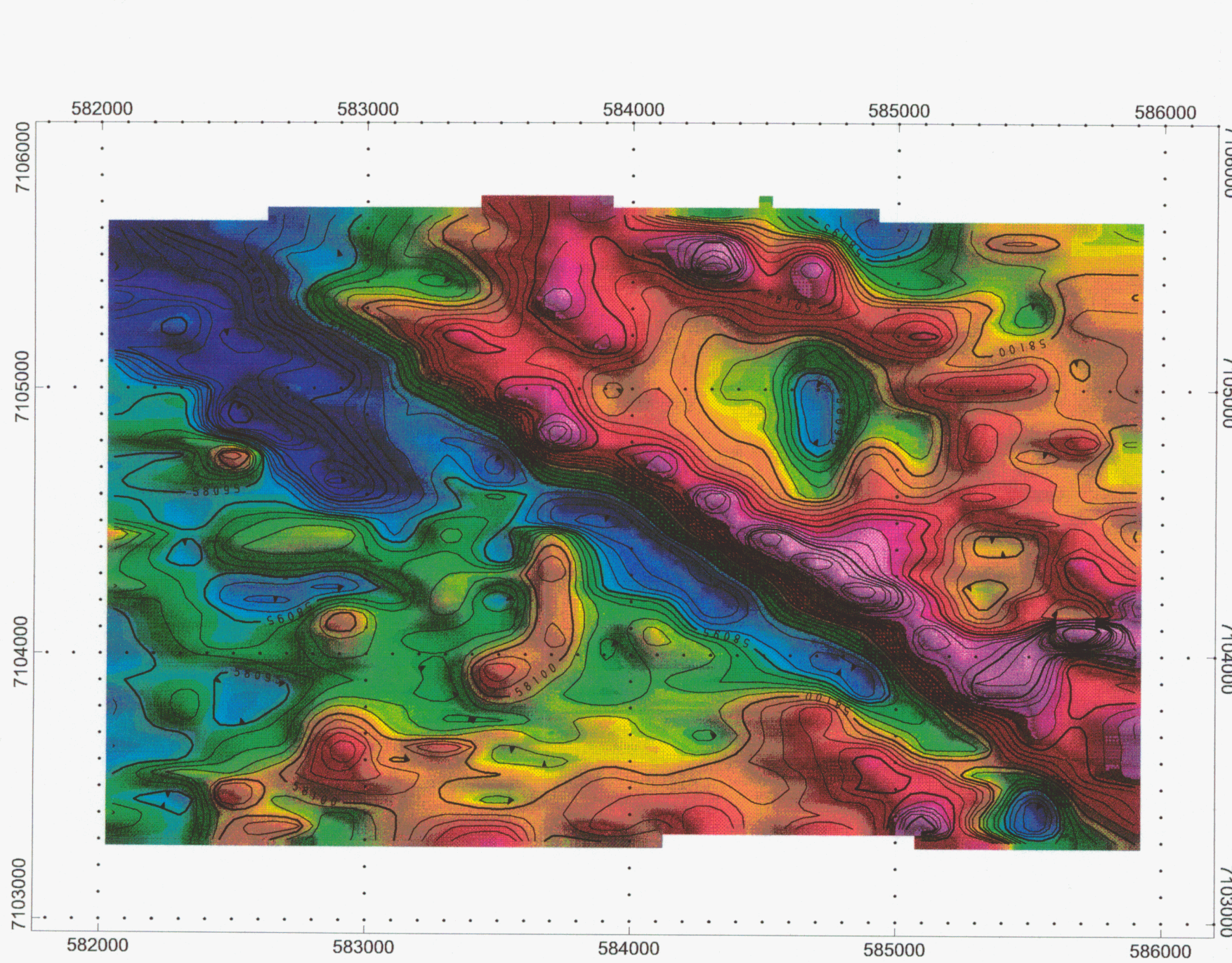




YUKON ENERGY, MINES  
& RESOURCES LIBRARY  
P.O. Box 2703  
Whitehorse, Yukon Y1A 2C8  
**094298**

MANSON CREEK REOURCES
TANNER CLAIM BLOCK CALCULATED VERTICAL GRADIENT
RC JAN 02

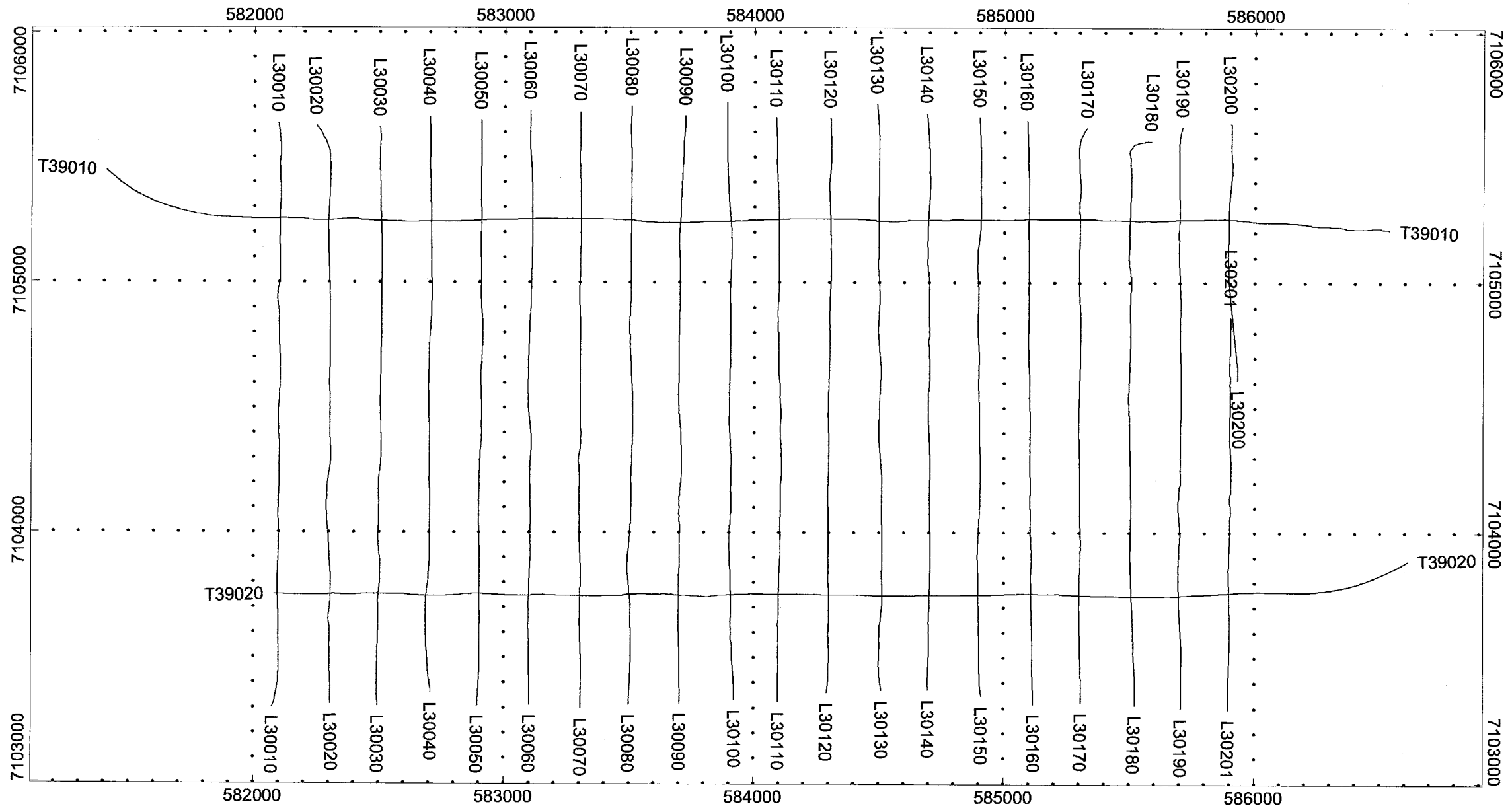


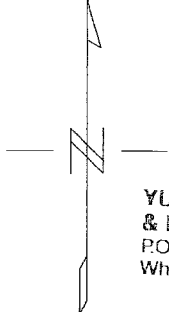


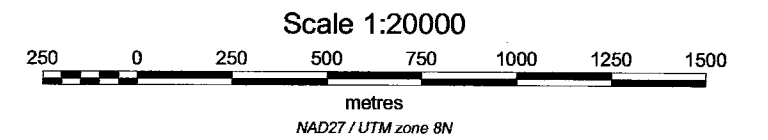
YUKON ENERGY, MINES  
& RESOURCES LIBRARY  
P.O. Box 2703  
Whitehorse, Yukon Y1A 2C8  
**094298**

<b>MANSON CREEK REOURCES</b>
<b>TANNER CLAIM BLOCK</b> <b>TOTAL FIELD MAGNETICS</b>
CONTOURS AT 1 AND 5nT
<b>RC JAN 02</b>





  
**YUKON ENERGY, MINES  
& RESOURCES LIBRARY**  
 P.O. Box 2703  
 Whitehorse, Yukon Y1A 2C6



094298

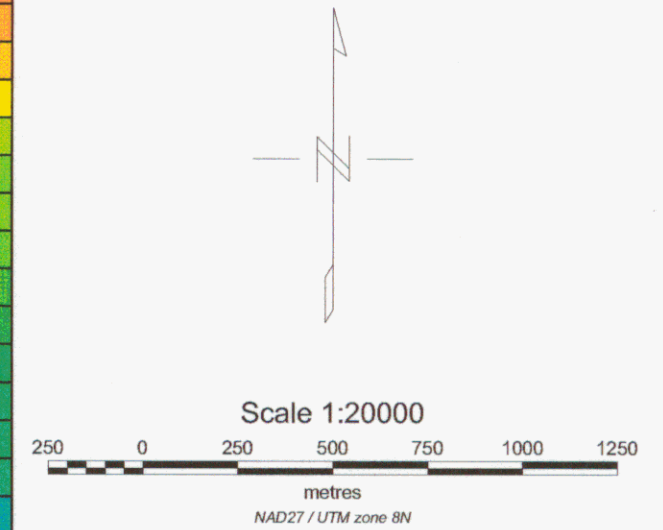
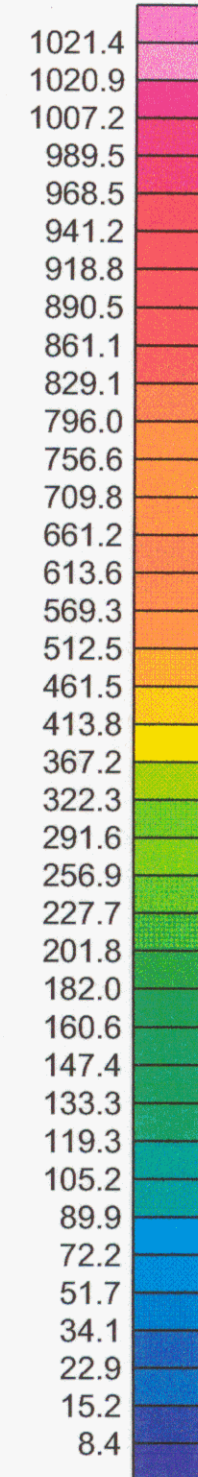
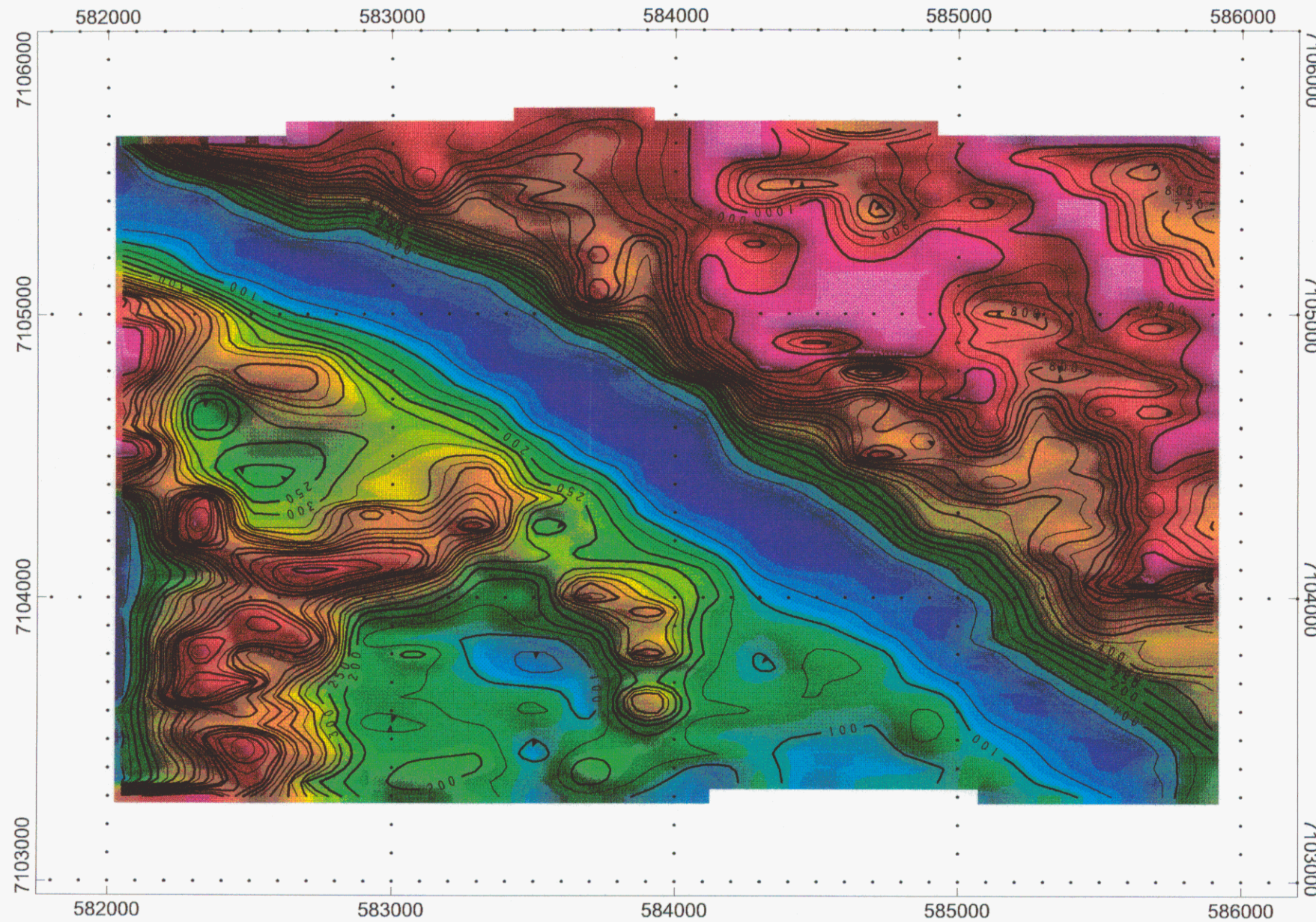
**MANSON CREEK REOURCES**

**TANNER CLAIM BLOCK  
FLIGHT LINE PATH**

**RC JAN 02**



YUKON ENERGY, MINES  
& RESOURCES LIBRARY  
P.O. Box 2703  
Whitehorse, Yukon Y1A 2C8

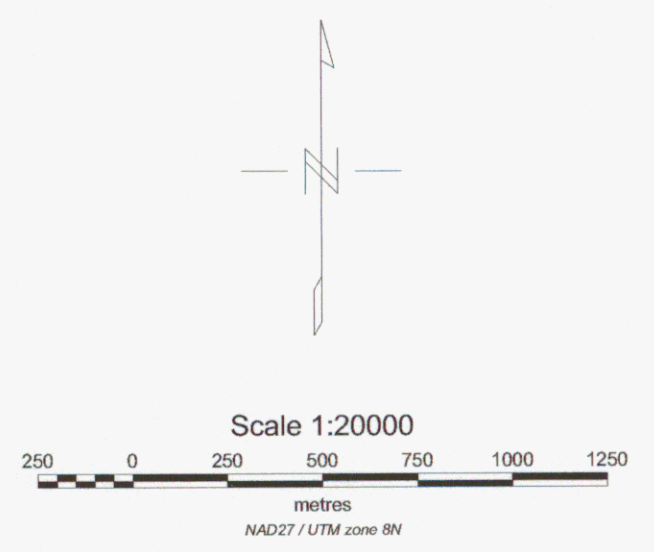
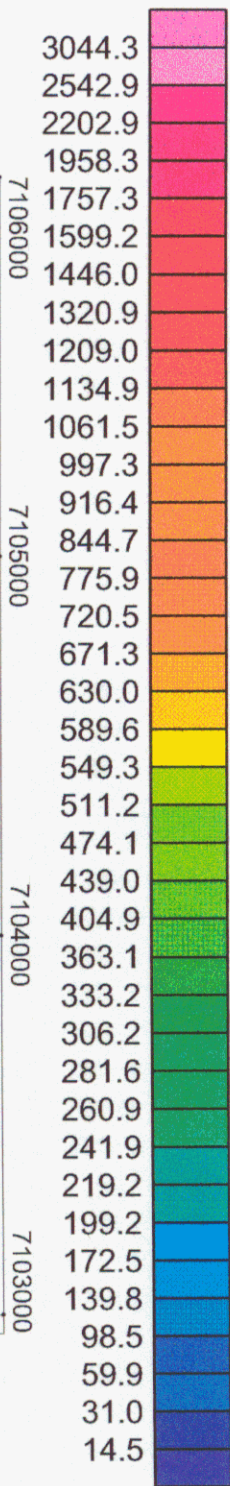
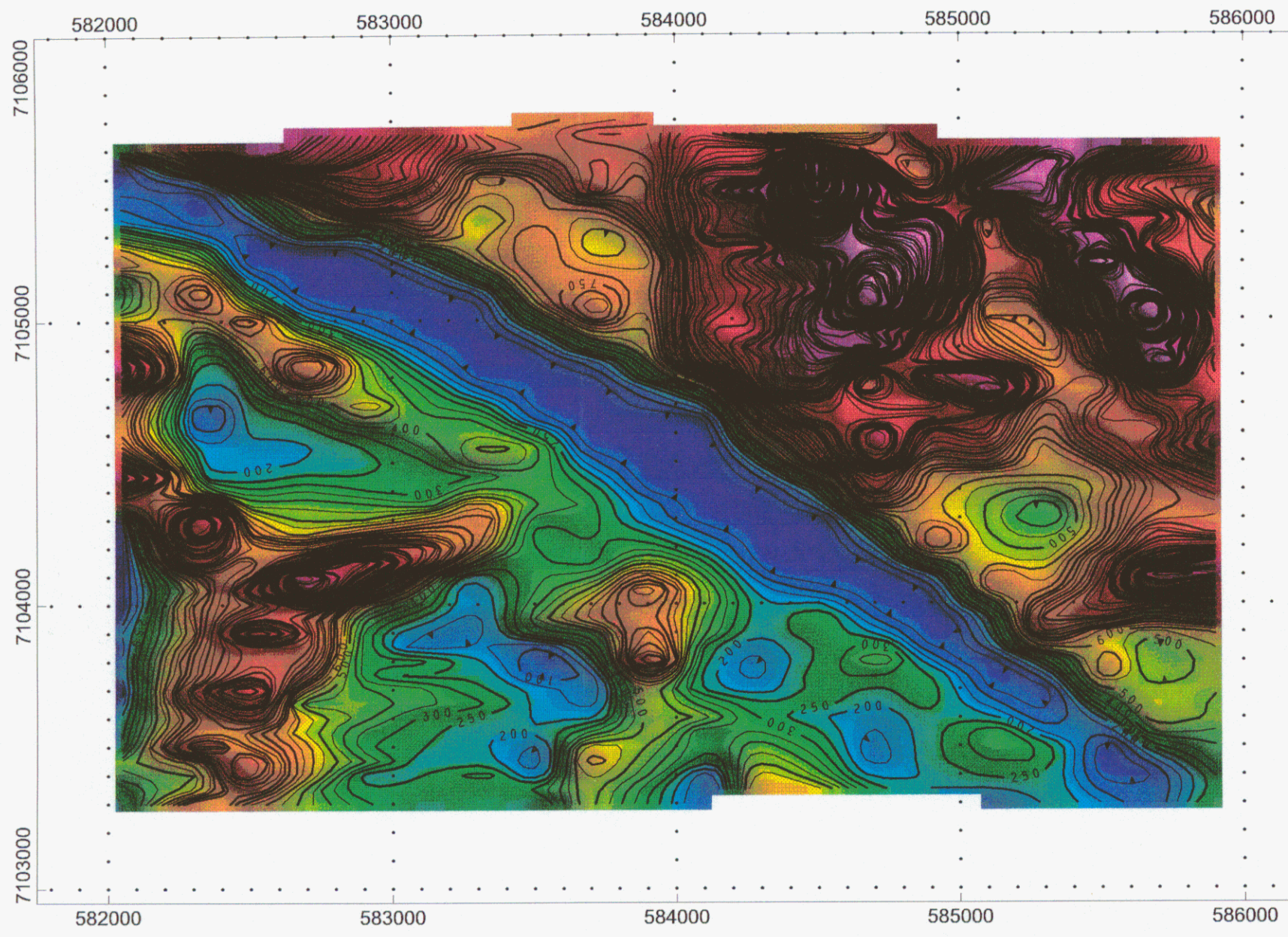


094298

<b>MANSON CREEK REOURCES</b>
<b>TANNER CLAIM BLOCK</b> <b>APPARENT RESISTIVITY 900 Hz</b> <b>UNITS - OHM-METER</b>
CONTOUR INTERVALS: 50, 100, 250 OHM-M
<b>RC JAN 02</b>



YUKON ENERGY, MINES  
& RESOURCES LIBRARY  
P.O. Box 2703  
Whitehorse, Yukon Y1A 2C8

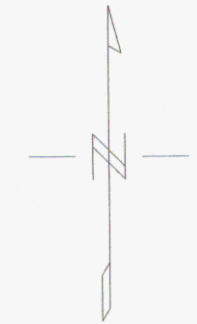
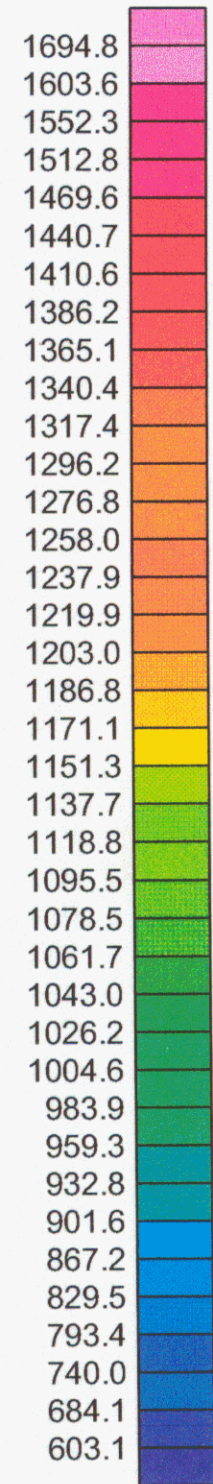
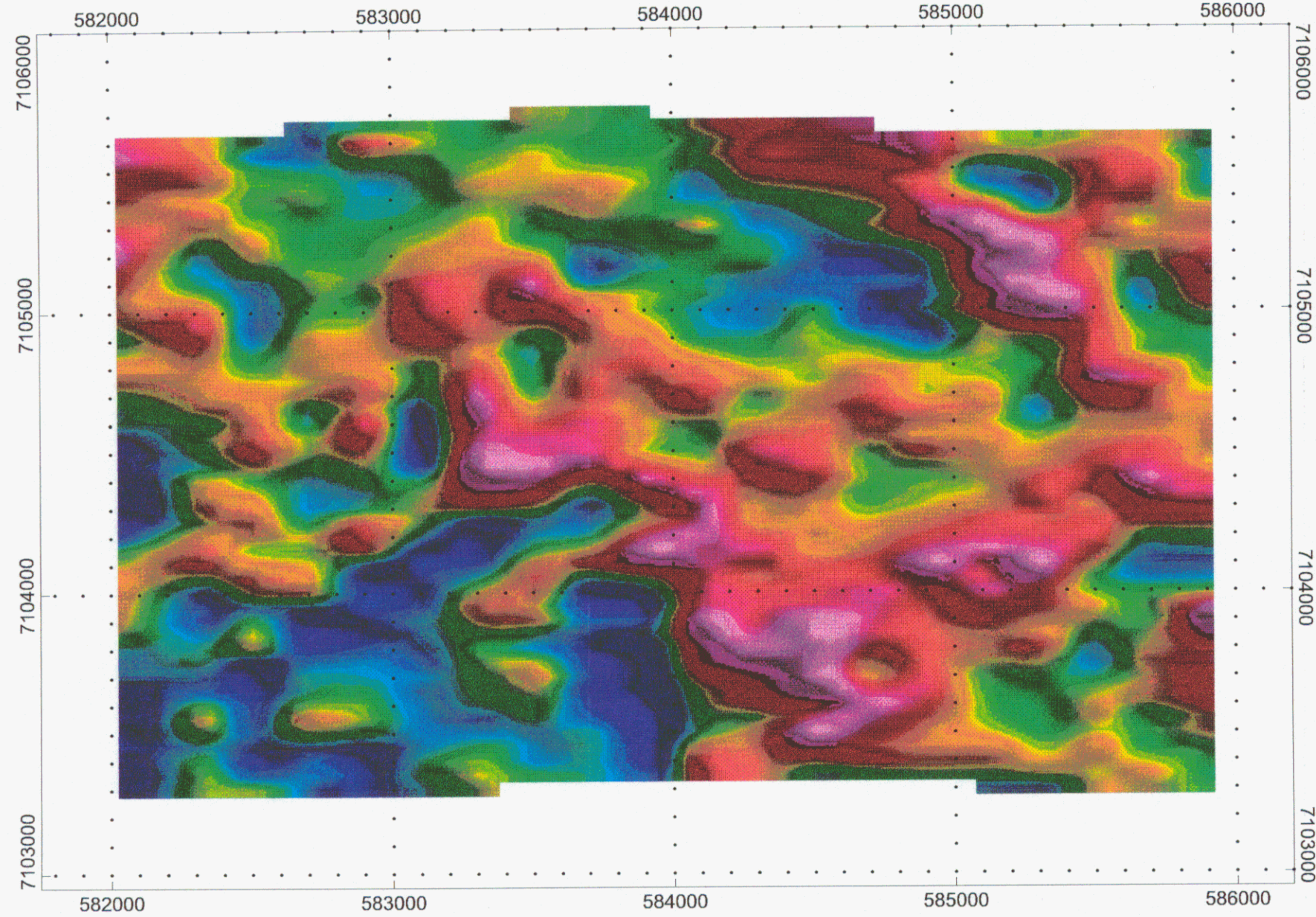


094298

<b>MANSON CREEK REOURCES</b>
<b>TANNER CLAIM BLOCK</b> <b>APPARENT RESISTIVITY 7200 Hz</b> <b>UNITS - OHM-METER</b>
CONTOUR INTERVALS: 50, 100, 250 OHM-M
<b>RC JAN 02</b>



YUKON ENERGY, MINES  
& RESOURCES LIBRARY  
P.O. Box 2703  
Whitehorse, Yukon Y1A 2C6

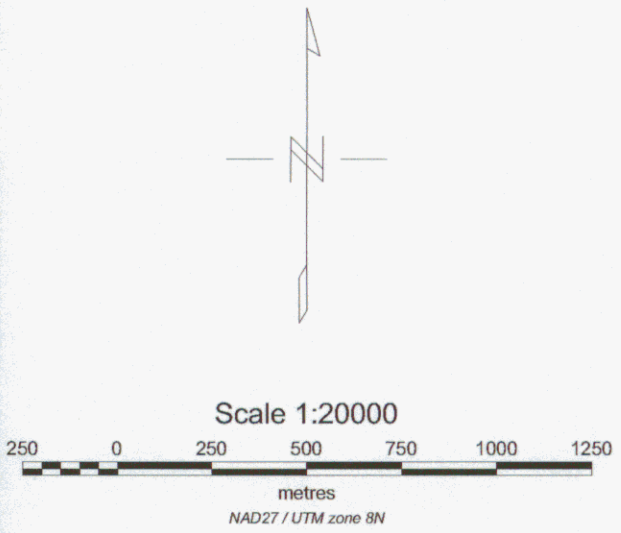
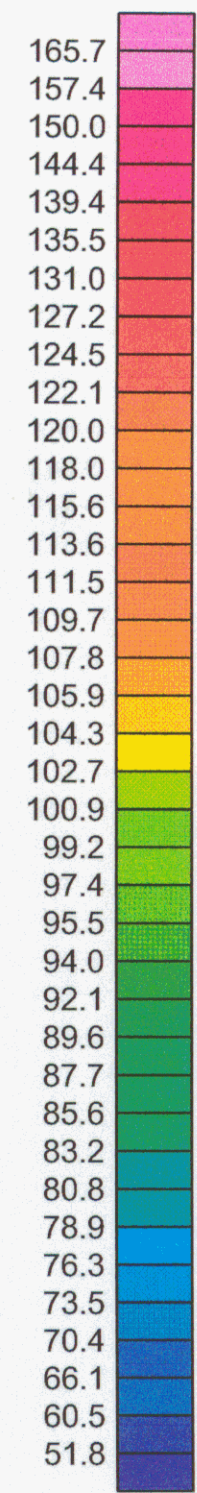
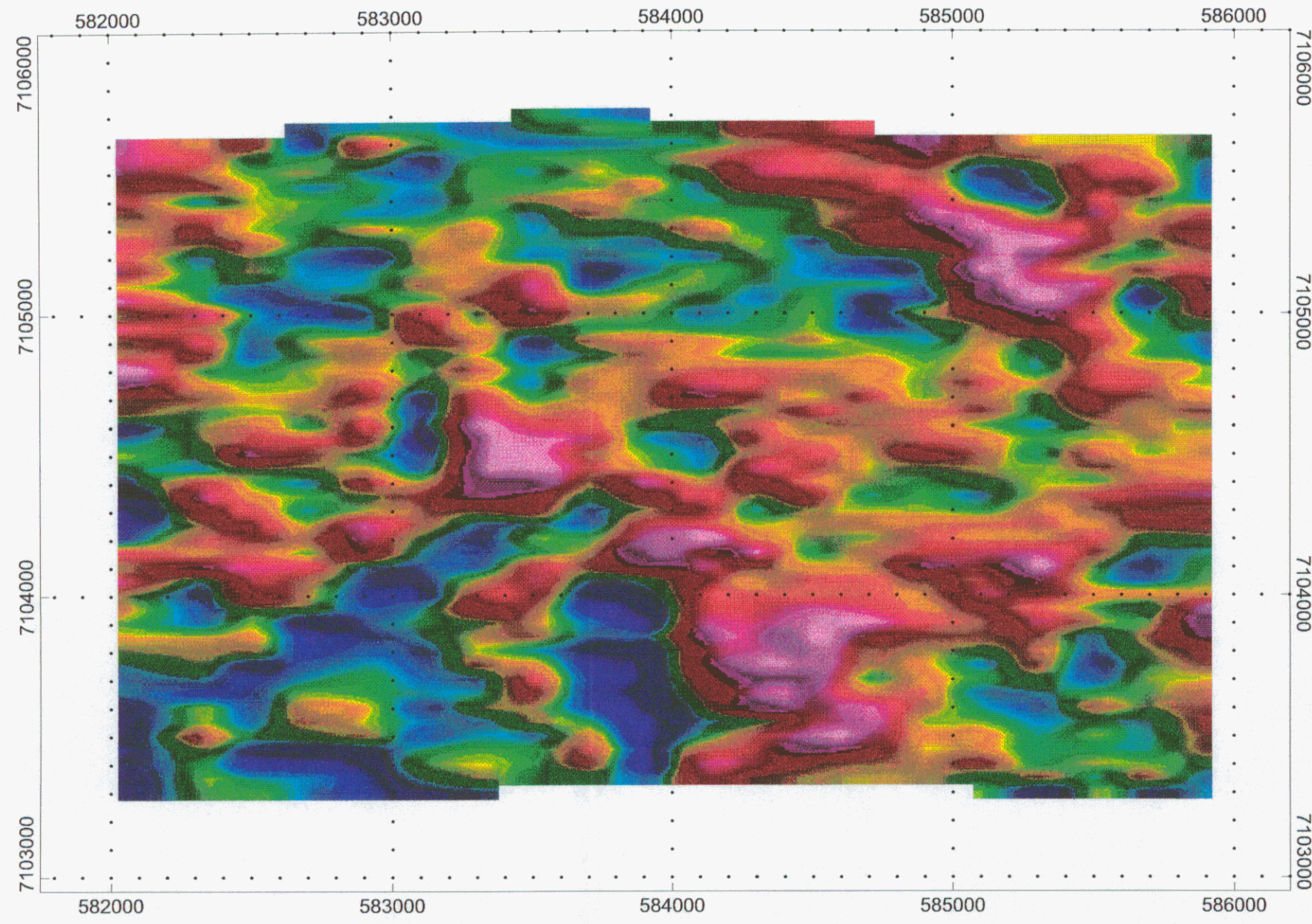


094298

<b>MANSON CREEK REOURCES</b>
<b>TANNER CLAIM BLOCK</b> Combined Total Count UNITS - CPS
<b>RC JAN 02</b>



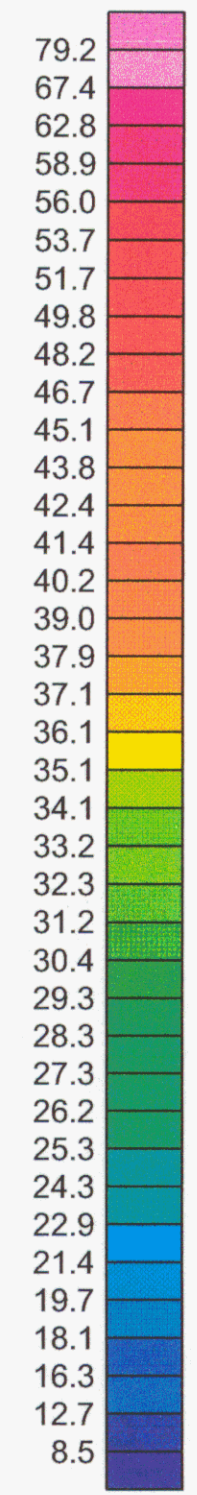
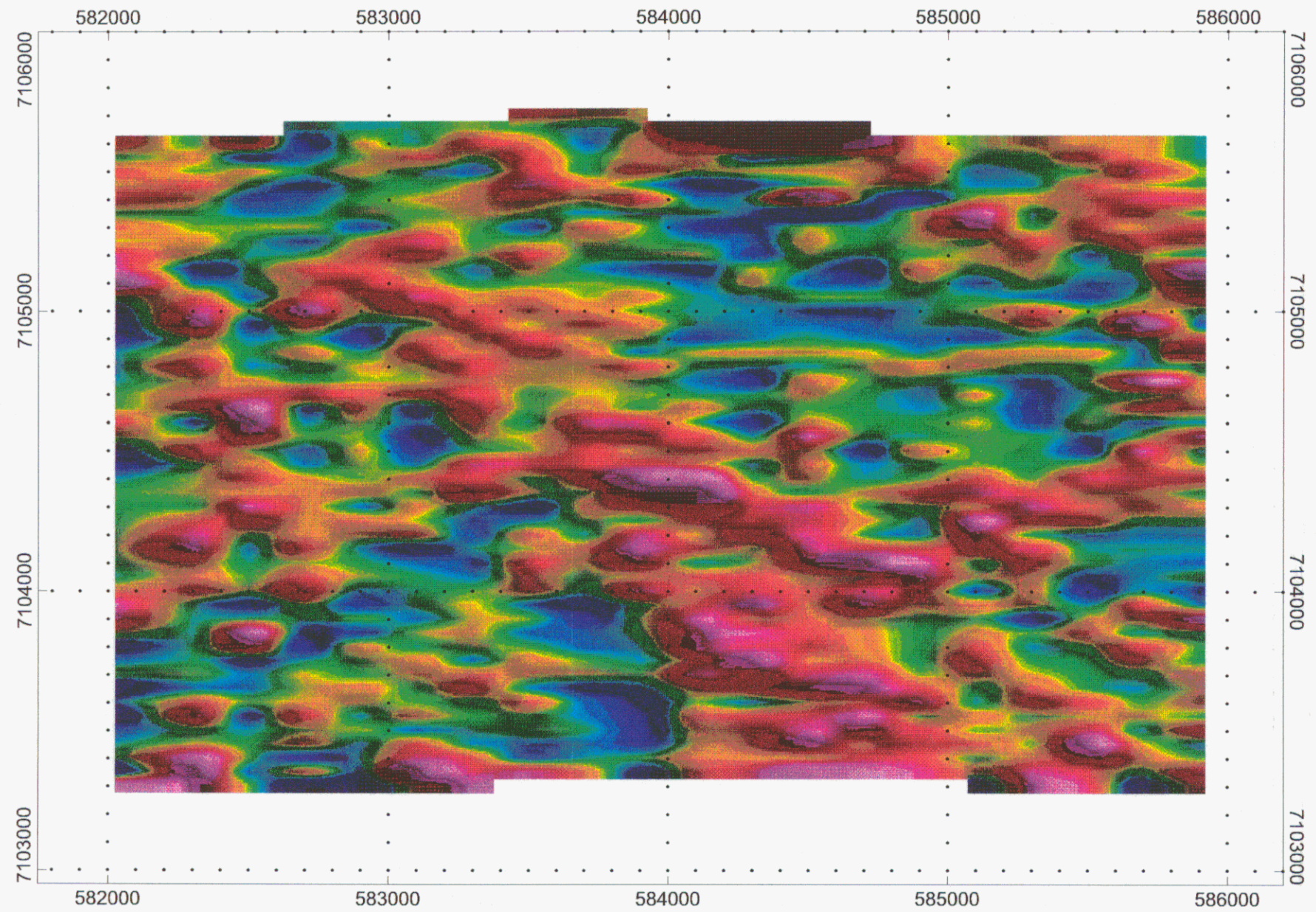
YUKON ENERGY, MINES  
& RESOURCES LIBRARY  
P.O. Box 2703  
Whitehorse, Yukon Y1A 2C6



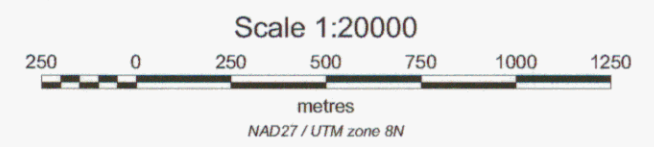
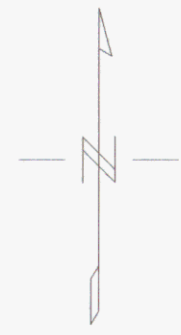
094298

MANSON CREEK REOURCES
TANNER CLAIM BLOCK POTASSIUM COUNT UNITS - CPS
RC JAN 02





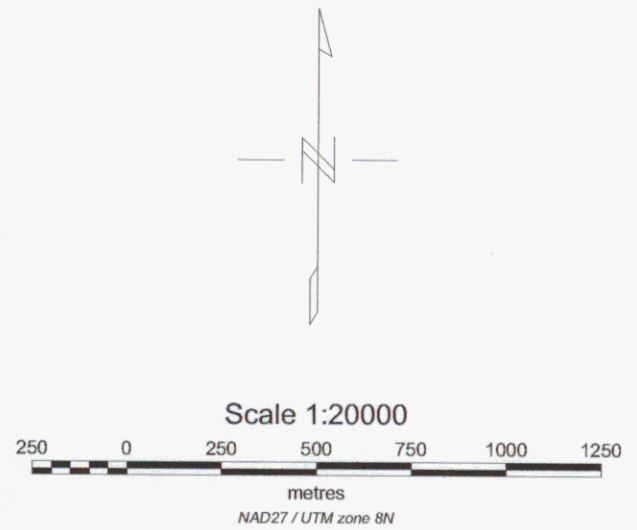
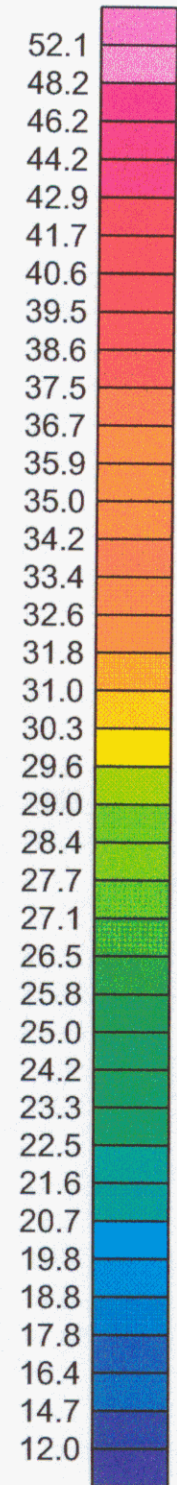
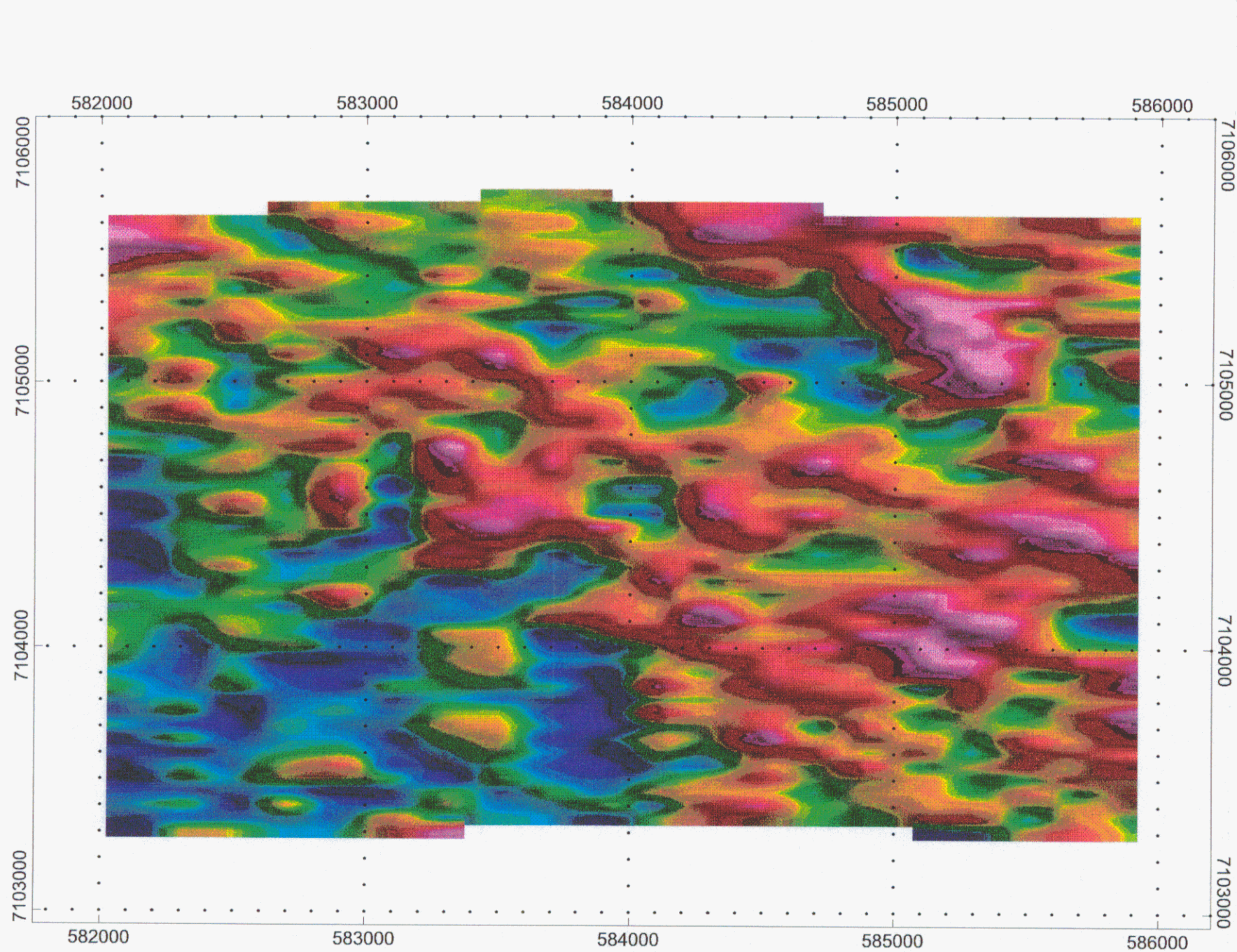
YUKON ENERGY, MINES  
& RESOURCES LIBRARY  
P.O. Box 2703  
Whitehorse, Yukon Y1A 2C8



094298

<b>MANSON CREEK REOURCES</b>
<b>TANNER CLAIM BLOCK</b> Uranium total count UNITS - CPS
<b>RC JAN 02</b>



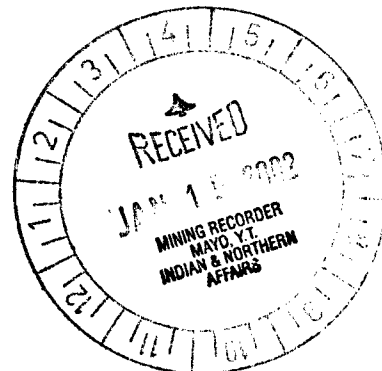


094298

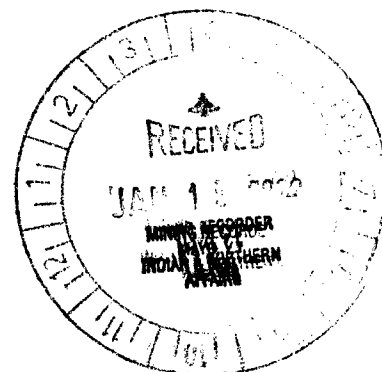
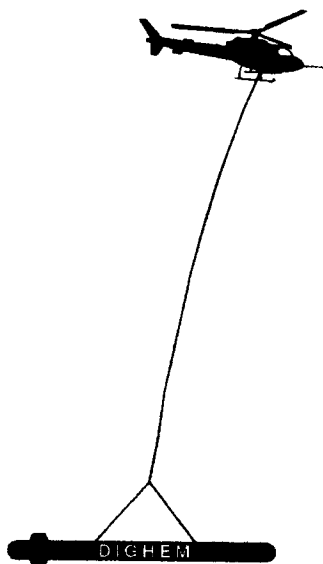
MANSON CREEK REOURCES
TANNER CLAIM BLOCK Thorium Total Count UNITS - CPS
RC JAN 02



DIGHEM<sup>V</sup> SURVEY  
FOR  
MANSON CREEK RESOURCES LTD.  
TANNER BLOCK  
YUKON TERRITORY



NTS 106C/3



094298 V.2

Fugro Airborne Surveys Corp.  
Mississauga, Ontario

Paul A. Smith  
Geophysicist

September 5, 2001

## SUMMARY

This report describes the logistics and results of a DIGHEM<sup>V</sup> airborne geophysical survey carried out for Manson Creek Resources Ltd., over the Tanner block located in the Nadaleen River area, Yukon Territory. Total coverage of the survey block amounted to 57 line km. The survey was flown from July 16, 2001.

The purpose of the survey was to detect zones of conductive mineralization and to provide information which could be used to map the geology and structure of the survey area. This was accomplished by using a DIGHEM<sup>V</sup> multi-coil, multi-frequency electromagnetic system, supplemented by a high sensitivity cesium magnetometer, and a 256 channel spectrometer.

The information from these sensors was processed to produce maps which display the magnetic, radiometric and conductive properties of the survey area. A GPS electronic navigation system ensured accurate positioning of the geophysical data with respect to the base maps. Visual flight path recovery techniques were used to confirm the location of the helicopter where visible topographic features could be identified on the ground.

The survey properties contain numerous anomalous features, some of which are considered to be of moderate to high priority as exploration targets. Many of the inferred bedrock conductors warrant further investigation using appropriate surface exploration techniques. Areas of interest may be assigned priorities on the basis of supporting geophysical, geochemical and/or geological information. After initial investigations have been carried out, it may be necessary to re-evaluate the remaining anomalies based on information acquired from the follow-up program.

# CONTENTS

1.	INTRODUCTION.....	1.1
2.	SURVEY EQUIPMENT .....	2.1
	Electromagnetic System.....	2.1
	Magnetometer.....	2.3
	Magnetic Base Stations .....	2.4
	Spectrometer.....	2.4
	Radar Altimeter .....	2.6
	Barometric Pressure and Temperature Sensors .....	2.6
	Analog Recorder .....	2.7
	Digital Data Acquisition System .....	2.7
	Video Flight Path Recording System.....	2.9
	Navigation (Global Positioning System) .....	2.9
	Field Workstation .....	2.11
3.	PRODUCTS AND PROCESSING TECHNIQUES.....	3.1
	Base Maps .....	3.1
	Electromagnetic Anomalies.....	3.3
	Apparent Resistivity .....	3.4
	EM Magnetite (optional) .....	3.5
	Total Magnetic Field.....	3.5
	Calculated Vertical Magnetic Gradient .....	3.5
	Magnetic Derivatives (optional) .....	3.6
	Radiometrics .....	3.6
	Pre-filtering .....	3.7
	Reduction to Standard Temperature and Pressure .....	3.7
	Live Time Correction.....	3.8
	Intermediate Filtering.....	3.8
	Aircraft and Cosmic Background .....	3.9
	Radon Background.....	3.9
	Compton Stripping.....	3.10
	Attenuation Corrections .....	3.11
	Multi-channel Stacked Profiles .....	3.12
	Contour, Colour and Shadow Map Displays.....	3.15
	Resistivity-depth Sections (optional) .....	3.15
4.	SURVEY RESULTS .....	4.1
	General Discussion .....	4.1
	Magnetics.....	4.3
	Apparent Resistivity .....	4.5
	Electromagnetic Anomalies.....	4.6
	Conductors in the Survey Areas.....	4.8
5.	CONCLUSIONS AND RECOMMENDATIONS.....	5.11

## **APPENDICES**

- A. List of Personnel
- B. Statement of Cost
- C. Background Information
- D. EM Anomaly List
- E. Radiometric Processing Control File/Coefficients
- F. Archive Description

## 1. INTRODUCTION

A DIGHEM<sup>V</sup> electromagnetic/resistivity/magnetic/radiometric survey was flown for Manson Creek Resources Ltd., on July 16, 2001, over the Tanner block in the Nadaleen River area, Yukon Territory. The survey area can be located on NTS map sheet 106C/3 (see Figures 1-3).

Survey coverage consisted of approximately 57 line-km, including tie lines. Flight lines were flown in an azimuthal direction of 180°/360° with a line separation of 200 metres. The block had two east/west tie lines (see Table 1-1).

The survey employed the DIGHEM<sup>V</sup> electromagnetic system. Ancillary equipment consisted of a magnetometer, radar and barometric altimeters, video camera, analog and digital recorders, a 256-channel spectrometer and an electronic navigation system. The instrumentation was installed in an AS350B2 turbine helicopter (Registration C-GBKV) which was provided by Questral Helicopters Ltd. The helicopter flew at an average airspeed of 68 km/h with an EM sensor height of approximately 30 metres. The spectrometer crystal package was housed within the helicopter, with a nominal terrain clearance of 60 m.

Section 2 provides details on the survey equipment, the data channels, their respective sensitivities, and the navigation/flight path recovery procedure. Noise levels of less than 2



ppm are generally maintained for wind speeds up to 35 km/h. Higher winds may cause the system to be grounded because excessive bird swinging produces difficulties in flying the helicopter. The swinging results from the 5 m<sup>2</sup> of area which is presented by the bird to broadside gusts.

**Table 1-1**

Block	Km	Direction	Flight #	Date
Tanner	57	N/S	3, 4	July 16

## 2. SURVEY EQUIPMENT

This section provides a brief description of the geophysical instruments used to acquire the survey data and the calibration procedures employed.

### Electromagnetic System

Model: DIGHEM<sup>V</sup>

Type: Towed bird, symmetric dipole configuration operated at a nominal survey altitude of 30 metres. Coil separation is 8 metres for 900 Hz, 5500 Hz and 7200 Hz, and 6.3 metres for the 56,000 Hz coil-pair.

Coil orientations/frequencies:	<u>orientation</u>	<u>nominal</u>	<u>actual</u>
	coaxial /	1,000 Hz	1,072 Hz
	coplanar /	900 Hz	888 Hz
	coaxial /	5,500 Hz	5,957 Hz
	coplanar /	7,200 Hz	7,248 Hz
	coplanar /	56,000 Hz	56,420 Hz

Channels recorded: 5 in-phase channels  
5 quadrature channels  
2 monitor channels

Sensitivity: 0.06 ppm at 1,000 Hz Cx  
0.12 ppm at 900 Hz Cp  
0.12 ppm at 5,500 Hz Cx  
0.24 ppm at 7,200 Hz Cp  
0.60 ppm at 56,000 Hz Cp

Sample rate: 10 per second, equivalent to 1 sample every 1.8 m, at a survey speed of 68 km/h.

The electromagnetic system utilizes a multi-coil coaxial/coplanar technique to energize conductors in different directions. The coaxial coils are vertical with their axes in the flight direction. The coplanar coils are horizontal. The secondary fields are sensed simultaneously by means of receiver coils which are maximum coupled to their respective transmitter coils. The system yields an in-phase and a quadrature channel from each transmitter-receiver coil-pair.

The Dighem calibration procedure involves four stages; primary field bucking, phase calibration, gain calibration, and zero adjust. At the beginning of the survey, the primary field at each receiver coil is cancelled, or "bucked out", by precise positioning of five bucking coils.

The phase calibration adjusts the phase angle of the receiver to match that of the transmitter. A ferrite bar, which produces a purely in-phase anomaly, is positioned near each receiver coil. The bar is rotated from minimum to maximum field coupling and the responses for the in-phase and quadrature components for each coil pair/frequency are measured. The phase of the response is adjusted at the console to return an in-phase only response for each coil-pair. Phase checks are performed daily.

The gain calibration uses external coils designed to produce an equal response on in-phase and quadrature components for each frequency/coil-pair. The coil parameters and distances are designed to produce pre-determined responses at the receiver, due to the current induced in the calibration coil by the transmitter when a switch closes the

loop at the coil. The gain at the console is adjusted to yield secondary responses of exactly 100 ppm (Cx) and 200 ppm (Cp). Gain calibrations are carried out at the beginning and end of the survey.

The phase and gain calibrations each measure a relative change in the secondary field, rather than an absolute value. This removes any dependency of the calibration procedure on the secondary field due to the ground, except under circumstances of extreme ground conductivity.

During each survey flight, internal (Q-coil) calibration signals are generated to recheck system gain and to establish zero reference levels. These calibrations are carried out at intervals of approximately 20 minutes with the system out of ground effect. At a sensor height of more than 250 m, there is no measurable secondary field from the earth. The remaining residual is therefore established as the zero level of the system. Linear system drift is automatically removed by re-establishing zero levels between the Q-coil calibrations.

## **Magnetometer**

Model:	Picodas MEP-710 processor with Geometrics G822 sensor
Type:	Optically pumped cesium vapour
Sensitivity:	0.01 nT
Sample rate:	10 per second

The magnetometer sensor is housed in the EM bird, 28 m below the helicopter.

## **Magnetic Base Stations**

Model: GEM Systems GSM-19T  
Type: Digital recording proton precession  
Sensitivity: 0.10 nT  
Sample rate: 0.2 per second

Model: Fugro CF-1 processor with Geometrics G823A sensor  
Type: Digital recording cesium vapour  
Sensitivity: 0.01 nT  
Sample rate: 1 per second

A digital recorder is operated in conjunction with the base station magnetometer to record the diurnal variations of the earth's magnetic field. The clock of the base station is synchronized with that of the airborne system to permit subsequent removal of diurnal drift.

## **Spectrometer**

Manufacturer: Exploranium  
Model: GR-820  
Type: 256 Multichannel, Potassium stabilized

Accuracy: 1 count/sec.  
Update: 1 integrated sample/sec.

The GR-820 Airborne Spectrometer employs four downward looking crystals (1024 cu.in.) and one upward looking crystal (256 cu.in.). The downward crystal records the radiometric spectrum from 410 KeV to 3 MeV over 256 discrete energy windows, as well as a cosmic ray channel which detects photons with energy levels above 3.0 MeV. From these 256 channels, the standard Total Count, Potassium, Uranium and Thorium channels are extracted. The upward crystal is used to measure and correct for Radon.

The shock-protected Sodium Iodide (Thallium) crystal package is unheated, and is automatically stabilized with respect to the Potassium peak. The GR-820 provides raw or Compton stripped data which has been automatically corrected for gain, base level, ADC offset and dead time.

The system is calibration before and after each flight using three accurately positioned hand-held sources. Additionally, fixed-site hover tests are carried out to determine if there are any differences in background. This procedure allows corrections to be applied to each survey flight, to eliminate any differences which might result from changes in temperature or humidity.

## **Radar Altimeter**

Manufacturer: Honeywell/Sperry  
Model: AA 300  
Type: Short pulse modulation, 4.3 GHz  
Sensitivity: 0.3 m

The radar altimeter measures the vertical distance between the helicopter and the ground. This information is used in the processing algorithm which determines conductor depth.

## **Barometric Pressure and Temperature Sensors**

Model: DIGHEM D 1300  
Type: Motorola MPX4115AP analog pressure sensor  
AD592AN high-impedance remote temperature sensors  
Sensitivity: Pressure: 150 mV/kPa  
Temperature: 100 mV/°C or 10 mV/°C (selectable)  
Sample rate: 10 per second

The D1300 circuit is used in conjunction with one barometric sensor and up to three temperature sensors. Two sensors (baro and temp) are installed in the EM console in the aircraft, to monitor pressure and internal operating temperatures. A third sensor is used to monitor temperature changes within the EM bird.

## **Analog Recorder**

Manufacturer: RMS Instruments  
Type: DGR33 dot-matrix graphics recorder  
Resolution: 4x4 dots/mm  
Speed: 1.5 mm/sec

The analog profiles are recorded on chart paper in the aircraft during the survey. Table 2-1 lists the geophysical data channels and the vertical scale of each profile.

## **Digital Data Acquisition System**

Manufacturer: RMS Instruments  
Model: DGR 33  
Recorder: 48 Mbyte flash card

The data are stored on a 48 Mbyte flash card and are downloaded to the field workstation PC at the survey base for verification, backup and preparation of in-field products.



**Table 2-1. The Analog Profiles**

Channel Name	Parameter	Scale units/mm	Designation on Digital Profile
1X9I	coaxial in-phase ( 1000 Hz)	2.5 ppm	CXI1000
1X9Q	coaxial quad ( 1000 Hz)	2.5 ppm	CXQ1000
3P9I	coplanar in-phase ( 900 Hz)	2.5 ppm	CPI900
3P9Q	coplanar quad ( 900 Hz)	2.5 ppm	CPQ900
2P7I	coplanar in-phase ( 7200 Hz)	5 ppm	CPI7200
2P7Q	coplanar quad ( 7200 Hz)	5 ppm	CPQ7200
4X7I	coaxial in-phase ( 5500 Hz)	5 ppm	CXI5500
4X7Q	coaxial quad ( 5500 Hz)	5 ppm	CXQ5500
5P5I	coplanar in-phase ( 56000 Hz)	10 ppm	CPI56K
5P5Q	coplanar quad ( 56000 Hz)	10 ppm	CPQ56K
ALTR	altimeter (radar)	3 m	ALTBIRD
MAGC	magnetics, coarse	20 nT	MAG50
MAGF	magnetics, fine	2.0 nT	MAG5
CXSP	coaxial sferics monitor		
CPSP	coplanar sferics monitor		CPSP
CXPL	coaxial powerline monitor		
CPPL	coplanar powerline monitor		CPPL
TC	total counts	100 cps	TC
K	potassium	10 cps	K
U	uranium	10 cps	U
TH	thorium	10 cps	TH
1KPA	altimeter (barometric)	30 m	
2TDC	internal (console) temperature	1° C	
3TDC	external temperature (EM bird)	1° C	

## **Video Flight Path Recording System**

Type: Panasonic VHS Colour Video Camera (NTSC)

Model: AG 2400/WVCD132

Fiducial numbers are recorded continuously and are displayed on the margin of each image. This procedure ensures accurate correlation of analog and digital data with respect to visible features on the ground.

## **Navigation (Global Positioning System)**

### Airborne Receiver

Model: Ashtech Glonass GG24

Type: SPS (L1 band), 24-channel, C/A code at 1575.42 MHz,  
S code at 0.5625 MHz, Real-time differential.

Sensitivity: -132 dBm, 0.5 second update

Accuracy: Manufacturer's stated accuracy is better than 10 metres  
real-time

### Base Station (CF-1)

Model: Marconi Alistar OEM, CMT-1200

Type: Code and carrier tracking of L1 band, 12-channel, C/A code  
at 1575.42 MHz

Sensitivity: -90 dBm, 1.0 second update

Accuracy: Manufacturer's stated accuracy for differential corrected GPS is 2 metres

The Ashtech GG24 is a line of sight, satellite navigation system which utilizes time-coded signals from at least four of forty-eight available satellites. Both Russian GLONASS and American NAVSTAR satellite constellations are used to calculate the position and to provide real time guidance to the helicopter. The Ashtech system can be combined with a RACAL or similar GPS receiver which further improves the accuracy of the flying and subsequent flight path recovery to better than 5 metres. The differential corrections, which are obtained from a network of virtual reference stations, are transmitted to the helicopter via a spot-beam satellite. This eliminates the need for a local GPS base station. However, the Marconi Allstar OEM (CMT-1200), part of the CF-1 base station, was used to provide post-survey differential corrections.

The Marconi Allstar utilizes time-coded signals from at least four of the twenty-four NAVSTAR satellites. The base station raw XYZ data are recorded, thereby permitting post-survey processing for theoretical accuracies of better than 5 metres.

The Ashtech receiver is coupled with a PNAV 2100 navigation system for real-time guidance. Navigation data are recorded on 48 Mbyte flash cards.

Although the base station receiver is able to calculate its own latitude and longitude, a higher degree of accuracy can be obtained if the reference unit is established on a known benchmark or triangulation point. For this survey, the GPS station was located at latitude 64°13.36773'N, longitude 133°13.11516'W at an ellipsoid elevation of 864.7 m. The GPS records data relative to the WGS84 ellipsoid, which is the basis of the revised North American Datum (NAD83). Conversion software is used to transform the WGS84 coordinates to the NAD27 UTM system displayed on the base maps.

### **Field Workstation**

A PC is used at the survey base to verify data quality and completeness. Flight data are transferred to the PC hard drive to permit the creation of a database using a proprietary software package (typhoon-version 17.01.04). This process allows the field operators to display both the positional (flight path) and geophysical data on a screen or printer.

### 3. PRODUCTS AND PROCESSING TECHNIQUES

Table 3-1 lists the maps and products which have been provided under the terms of the survey agreement. Other products can be prepared from the existing dataset, if requested.

These include magnetic enhancements or derivatives, percent magnetite, digital terrain or resistivity-depth sections. Most parameters can be displayed as contours, profiles, or in colour.

#### Base Maps

Base maps of the survey area have been produced from published topographic maps. These provide a relatively accurate, distortion-free base which facilitates correlation of the navigation data to the UTM grid. The original topographic maps are scanned to a bitmap format and combined with geophysical data for plotting the final maps. All maps are created using the following parameters:

#### Projection Description:

Datum:	NAD27 (Yukon)
Ellipsoid:	Clarke 1866
Projection:	UTM (Zone: 8)
Central Meridian:	135°W
False Northing:	0
False Easting:	500000
Scale Factor:	0.9996
WGS84 to Local Conversion:	Molodensky
Datum Shifts:	DX: +7    DY: -139    DZ: -181

### Table 3-1 Survey Products

1. Final Transparent Maps (+3 prints) @ 1:10,000

Dighem EM anomalies  
Total magnetic field  
Calculated vertical magnetic gradient  
Apparent resistivity (900 Hz)  
Apparent resistivity (7200 Hz)

2. Colour Maps (2 sets) @ 1:10,000

Total magnetic field  
Calculated vertical magnetic gradient  
Apparent resistivity (900 Hz)  
Apparent resistivity (7200 Hz)  
Radiometrics – Total Count  
Radiometrics – Potassium  
Radiometrics – Uranium  
Radiometrics – Thorium

3. Additional Products

Digital XYZ archive in Geosoft ASCII format (CD-ROM)  
Digital grid archives in Geosoft GRD format (CD-ROM)  
Survey report (3 copies)  
Multi-channel stacked profiles  
Analog chart records  
Flight path video cassettes

Note: Other products can be produced from existing survey data, if requested.

## **Electromagnetic Anomalies**

EM data are processed at the recorded sample rate of 10 samples/second. If necessary, appropriate spheric rejection median or Hanning filters are applied to reduce noise to acceptable levels. EM test profiles are then created to allow the interpreter to select the most appropriate EM anomaly picking controls for a given survey area. The EM picking parameters depend on several factors but are primarily based on the dynamic range of the resistivities within the survey area, and the types and expected geophysical responses of the targets being sought.

Anomalous electromagnetic responses are selected and analysed by computer to provide a preliminary electromagnetic anomaly map. The automatic selection algorithm is intentionally oversensitive to assure that no meaningful responses are missed. Using the preliminary map in conjunction with the multi-parameter stacked profiles, the interpreter then classifies the anomalies according to their source and eliminates those that are not substantiated by the data. The final interpreted EM anomaly map includes bedrock, surficial and cultural conductors. A map containing only bedrock conductors can be generated, if desired.

## **Apparent Resistivity**

The apparent resistivity in ohm-m can be generated from the in-phase and quadrature EM components for any of the frequencies, using a pseudo-layer half-space model. A resistivity map portrays all the EM information for that frequency over the entire survey area. This contrasts with the electromagnetic anomaly map which provides information only over interpreted conductors. The large dynamic range makes the resistivity parameter an excellent mapping tool.

The preliminary resistivity maps and images are carefully inspected to locate any lines or line segments which might require levelling adjustments. Subtle changes between in-flight calibrations of the system can result in line to line differences, particularly in resistive (low signal amplitude) areas. If required, manual levelling is carried out to eliminate or minimize resistivity differences which can be caused by changes in operating temperatures. These levelling adjustments are usually very subtle, and do not result in the degradation of anomalies from valid bedrock sources.

After the manual levelling process is complete, revised resistivity grids are created. The resulting grids can be subjected to a microlevelling filter in order to smooth the data for contouring. The coplanar resistivity parameter has a broad 'footprint' which requires very little filtering.



The calculated resistivities for the three coplanar frequencies are included in the XYZ and grid archives. Values are in ohm-metres on all final products.

### **EM Magnetite (optional)**

The apparent percent magnetite by weight is computed wherever magnetite produces a negative in-phase EM response. This calculation is more meaningful in resistive areas.

### **Total Magnetic Field**

The aeromagnetic data are corrected for diurnal variation using the magnetic base station data. Manual adjustments are applied to any lines that require levelling, as indicated by shadowed images of the gridded magnetic data or tie line/traverse line intercepts. The IGRF gradient can be removed from the corrected total field data, if requested.

### **Calculated Vertical Magnetic Gradient**

The diurnally-corrected total magnetic field data are subjected to a processing algorithm which enhances the response of magnetic bodies in the upper 500 m and attenuates the response of deeper bodies. The resulting vertical gradient map provides better definition and resolution of near-surface magnetic units. It also identifies weak magnetic features

which may not be evident on the total field map. However, regional magnetic variations and changes in lithology may be better defined on the total magnetic field map.

### **Magnetic Derivatives (optional)**

The total magnetic field data can be subjected to a variety of filtering techniques to yield maps of the following:

- enhanced magnetics
- second vertical derivative
- reduction to the pole/equator
- magnetic susceptibility with reduction to the pole
- upward/downward continuations
- analytic signal

All of these filtering techniques improve the recognition of near-surface magnetic bodies, with the exception of upward continuation. Any of these parameters can be produced on request. Dighem's proprietary enhanced magnetic technique is designed to provide a general "all-purpose" map, combining the more useful features of the above parameters.

### **Radiometrics**

All radiometric data reductions performed by Fugro rigorously follow the procedures described in the IAEA Technical Report<sup>1</sup>.

---

<sup>1</sup> Exploranium, I.A.E.A. Report, Airborne Gamma-Ray Spectrometer Surveying, Technical Report No. 323, 1991.

All processing of radiometric data was undertaken at the natural sampling rate of the spectrometer, i.e., one second. The data were not interpolated to match the fundamental 0.1 second interval of the EM and magnetic data.

The following sections describe each step in the process.

#### **Pre-filtering**

The radar altimeter data were processed with a 25-point median filter to remove spikes, followed by a 25-point Hanning filter.

#### **Reduction to Standard Temperature and Pressure**

The radar altimeter data were converted to effective height ( $h_e$ ) in feet using the acquired temperature and pressure data, according to the following formula:

$$h_e = h * \frac{273.15}{T + 273.15} * \frac{P}{1013.25}$$

where:  $h$  is the observed crystal to ground distance in feet

$T$  is the measured air temperature in degrees Celsius

$P$  is the barometric pressure in millibars

### Live Time Correction

The spectrometer, an Exploranium GR-820, uses the notion of "live time" to express the relative period of time the instrument was able to register new pulses per sample interval. This is the opposite of the traditional "dead time", which is an expression of the relative period of time the system was unable to register new pulses per sample interval.

The GR-820 measures the live time electronically, and outputs the value in milliseconds. The live time correction is applied to the total count, potassium, uranium, thorium, upward uranium and cosmic channels. The formula used to apply the correction is as follows:

$$C_{lt} = C_{raw} * \frac{1000.0}{L}$$

where:  $C_{lt}$  is the live time corrected channel in counts per second

$C_{raw}$  is the raw channel data in counts per second

$L$  is the live time in milliseconds

### Intermediate Filtering

Two parameters were filtered, but not returned to the database:

- Radar altimeter was smoothed with a 5-point Hanning filter ( $h_{ef}$ ).
- The Cosmic window was smoothed with a 29-point Hanning filter ( $Cos_f$ ).

### **Aircraft and Cosmic Background**

Aircraft background and cosmic stripping corrections were applied to the total count, potassium, uranium, thorium and upward uranium channels using the following formula:

$$C_{ac} = C_{lt} - (a_c + b_c * Cos_f)$$

- where:
- $C_{ac}$  is the background and cosmic corrected channel
  - $C_{lt}$  is the live time corrected channel
  - $a_c$  is the aircraft background for this channel
  - $b_c$  is the cosmic stripping coefficient for this channel
  - $Cos_f$  is the filtered Cosmic channel

### **Radon Background**

The determination of calibration constants that enable the stripping of the effects of atmospheric radon from the downward-looking detectors is accomplished through the use of an upward-looking detector. However, for this survey, radon corrections were negligible, and were not applied to the data.

A test line was established near the survey area. The tests were carried out at the start and end of each day, and at the end of the survey (July 17). Data were acquired over a four minute period at the nominal survey altitude (60 m). The data were then corrected for livetime, aircraft background and cosmic activity.

Once the survey was completed, the relationships between the counts in the downward uranium window and in the other four windows due to atmospheric radon were determined using linear regression.

### **Compton Stripping**

Following the radon correction, the potassium, uranium and thorium are corrected for spectral overlap. First  $\alpha$ ,  $\beta$ , and  $\gamma$  the stripping ratios, are modified according to altitude. Then an adjustment factor based on  $\alpha$ , the reversed stripping ratio, uranium into thorium, is calculated. (Note: the stripping ratio altitude correction constants are expressed in change per metre. A constant of 0.3048 is required to conform to the internal usage of height in feet):

$$\alpha_h = \alpha + h_{ef} * 0.00049$$

$$\beta_h = \beta + h_{ef} * 0.00065$$

$$\gamma_h = \gamma + h_{ef} * 0.00069$$

where:  $\alpha, \beta, \gamma$  are the Compton stripping coefficients

$\alpha_h, \beta_h, \gamma_h$  are the height corrected Compton stripping coefficients

$h_{ef}$  is the height above ground in metres

The stripping corrections are then carried out using the following formulas:

$$\alpha_r = \frac{1}{1 - a\alpha_h - g\gamma_h + ag\beta_h}$$

$$Th_c = ((1 - g\gamma_h)Th_{rc} - aU_{rc} + agk_{rc}) * \alpha_r$$

$$U_c = (Th_{rc}(g\beta_h - \alpha_h) + U_{rc} - K_{rc}^s) * \alpha_r$$

$$K_c = (Th_{rc}(a\alpha_h - \beta_h) + U_{rc}(a\beta_h - \gamma_h) + K_{rc}(1 - a\alpha_h)) * \alpha_r$$

where:  $U_c, Th_c$  and  $K_c$  are corrected uranium, thorium and potassium

$\alpha_h, \beta_h, \gamma_h$  are the height corrected Compton stripping coefficients

$U_{rc}, Th_{rc}$  and  $K_{rc}$  are radon-corrected uranium, thorium and potassium

$\alpha_r$  is the backscatter correction

$a$  is the reverse stripping ratio U into Th

$g$  is the reverse stripping ratio K into uranium

### Attenuation Corrections

The total count, potassium, uranium and thorium data are then corrected to a nominal survey altitude, in this case 200 feet. This is done according to the equation:

$$C_a = C * e^{\mu(h_{ef}-h_0)}$$

where:  $C_a$  is the output altitude corrected channel  
 $C$  is the input channel  
 $e^{\mu}$  is the attenuation correction for that channel  
 $h_{ef}$  is the effective altitude  
 $h_0$  is the nominal survey altitude to correct to

All coefficients used in processing the radiometric data are included in the Radiometric Processing Control Files appended to this report.

### **Multi-channel Stacked Profiles**

Distance-based profiles of the digitally recorded geophysical data are generated and plotted by computer. These profiles also contain the calculated parameters which are used in the interpretation process. These are produced as worksheets prior to interpretation, and are also presented in the final corrected form after interpretation. The profiles display electromagnetic anomalies with their respective interpretive symbols. Table 3-2 shows the parameters and scales for the multi-channel stacked profiles.



In Table 3-2, the log resistivity scale of 0.06 decade/mm means that the resistivity changes by an order of magnitude in 16.6 mm. The resistivities at 0, 33 and 67 mm up from the bottom of the digital profile are respectively 1, 100 and 10,000 ohm-m.

**Table 3-2. Multi-channel Stacked Profiles**

Channel Name (Freq)	Observed Parameters	Scale Units/mm
MAG5	total magnetic field (fine)	5 nT
MAG50	total magnetic field (coarse)	50 nT
BIRDHITE	EM sensor height above ground	6 m
ALTB	barometric altimeter (aircraft)	6 m
CXI900	vertical coaxial coil-pair in-phase (900 Hz)	5 ppm
CXQ900	vertical coaxial coil-pair quadrature (900 Hz)	5 ppm
CPI900	horizontal coplanar coil-pair in-phase (900 Hz)	10 ppm
CPQ900	horizontal coplanar coil-pair quadrature (900 Hz)	10 ppm
CXI5500	vertical coaxial coil-pair in-phase (5500 Hz)	10 ppm
CXQ5500	vertical coaxial coil-pair quadrature (5500 Hz)	10 ppm
CPI7200	horizontal coplanar coil-pair in-phase (7200 Hz)	20 ppm
CPQ7200	horizontal coplanar coil-pair quadrature (7200 Hz)	20 ppm
CPI56K	horizontal coplanar coil-pair in-phase (56,000 Hz)	40 ppm
CPQ56K	horizontal coplanar coil-pair quadrature (56,000 Hz)	40 ppm
CPPL	coplanar powerline monitor	
CPSP	coplanar spherics monitor	
	Computed Parameters	
DIFI ( 7200 Hz)	difference function in-phase from CXI and CPI	20 ppm
DIFQ ( 7200 Hz)	difference function quadrature from CXQ and CPQ	20 ppm
RES900	log resistivity	.06 decade
RES7200	log resistivity	.06 decade
RES56K	log resistivity	.06 decade
DP900	apparent depth	6 m
DP7200	apparent depth	6 m
DP56K	apparent depth	6 m
CDT	Conductance	1 grade

## **Contour, Colour and Shadow Map Displays**

The geophysical data are interpolated onto a regular grid using a modified Akima spline technique. The resulting grid is suitable for generating contour maps of excellent quality.

The grid cell size is usually 25% of the line interval.

Colour maps are produced by interpolating the grid down to the pixel size. The parameter is then incremented with respect to specific amplitude ranges to provide colour "contour" maps. Colour maps of the total magnetic field are particularly useful in defining the lithology of the survey area.

Monochromatic shadow maps or images are generated by employing an artificial sun to cast shadows on a surface defined by the geophysical grid. There are many variations in the shadowing technique. These techniques can be applied to total field or enhanced magnetic data, magnetic derivatives, VLF, resistivity, etc. The shadow of the enhanced magnetic parameter is particularly suited for defining geological structures with crisper images and improved resolution.

## **Resistivity-depth Sections (optional)**

The apparent resistivities for all frequencies can be displayed simultaneously as coloured resistivity-depth sections. Usually, only the coplanar data are displayed as the close

frequency separation between the coplanar and adjacent coaxial data tends to distort the section. The sections can be plotted using the topographic elevation profile as the surface. The digital terrain values, in metres a.m.s.l., can be calculated from the GPS z-value or barometric altimeter, minus the aircraft radar altimeter.

Resistivity-depth sections can be generated in three formats:

- (1) Sengpiel resistivity sections, where the apparent resistivity for each frequency is plotted at the depth of the centroid of the in-phase current flow<sup>2</sup>; and,
- (2) Differential resistivity sections, where the differential resistivity is plotted at the differential depth.
- (3) Occam<sup>4</sup> or Multi-layer<sup>5</sup> inversion.

Both the Sengpiel and differential methods are derived from the pseudo-layer half-space model. Both yield a coloured resistivity-depth section which attempts to portray a smoothed approximation of the true resistivity distribution with depth. Resistivity-depth sections are most useful in conductive layered situations, but may be unreliable in areas of

---

<sup>2</sup> Sengpiel, K.P., 1988, Approximate Inversion of Airborne EM Data from Multilayered Ground: *Geophysical Prospecting* 36, 446-459.

<sup>3</sup> Huang, H. and Fraser, D.C., 1993, Differential Resistivity Method for Multi-frequency Airborne EM Sounding: presented at Intern. Airb. EM Workshop, Tucson, Ariz.

<sup>4</sup> Constable et al, 1987, Occam's inversion: a practical algorithm for generating smooth models from electromagnetic sounding data: *Geophysics*, 52, 289-300.

<sup>5</sup> Huang H., and Palacky, G.J., 1991, Damped least-squares inversion of time domain airborne EM data based on singular value decomposition: *Geophysical Prospecting*, 39, 827-844.

moderate to high resistivity where signal amplitudes are weak. In areas where in-phase responses have been suppressed by the effects of magnetite, the computed resistivities shown on the sections may be unreliable.

Both the Occam and Multi-layer Inversions compute the layered earth resistivity model which would best match the measured EM data. The Occam inversion uses a series of thin, fixed layers (usually 20 x 5m and 10 x 10m layers) and computes resistivities to fit the EM data. The multi-layer inversion computes the resistivity and thickness for each of a defined number of layers (typically 3-5 layers) to best fit the data.

## 4. SURVEY RESULTS

### General Discussion

The survey results are presented on separate map sheets for each parameter at a scale of 1:20,000. Tables 4-1 summarizes the EM responses in the survey area, with respect to conductance grade and interpretation.

The anomalies shown on the electromagnetic anomaly maps are based on a near-vertical, half plane model. This model best reflects "discrete" bedrock conductors. Wide bedrock conductors or flat-lying conductive units, whether from surficial or bedrock sources, may give rise to very broad anomalous responses on the EM profiles. These may not appear on the electromagnetic anomaly map if they have a regional character rather than a locally anomalous character. These broad conductors, which more closely approximate a half-space model, will be maximum coupled to the horizontal (coplanar) coil-pair and should be more evident on the resistivity parameter. Resistivity maps, therefore, may be more valuable than the electromagnetic anomaly maps, in areas where broad or flat-lying conductors are considered to be of importance. Contoured resistivity maps, based on the 900 Hz and 7200 Hz coplanar data are included with this report.

**TABLE 4-1 EM ANOMALY STATISTICS  
TANNER BLOCK**

CONDUCTOR GRADE	CONDUCTANCE RANGE SIEMENS (MHOS)	NUMBER OF RESPONSES
7	>100	0
6	50 - 100	2
5	20 - 50	1
4	10 - 20	8
3	5 - 10	27
2	1 - 5	33
1	<1	40
*	INDETERMINATE	11
TOTAL		122

CONDUCTOR MODEL	MOST LIKELY SOURCE	NUMBER OF RESPONSES
D	DISCRETE BEDROCK CONDUCTOR	34
B	DISCRETE BEDROCK CONDUCTOR	45
S	CONDUCTIVE COVER	19
H	ROCK UNIT OR THICK COVER	14
E	EDGE OF WIDE CONDUCTOR	10
TOTAL		122

(SEE EM MAP LEGEND FOR EXPLANATIONS)

Excellent resolution and discrimination of conductors was accomplished by using a fast sampling rate of 0.1 sec and by employing a common frequency (5500 Cx/7200 Cp) on two orthogonal coil-pairs (coaxial and coplanar). The resulting "difference channel" parameters often permit differentiation of bedrock and surficial conductors, even though they may exhibit similar conductance values.

Anomalies which occur near the ends of the survey lines (i.e., outside the survey area), should be viewed with caution. Some of the weaker anomalies could be due to aerodynamic noise, i.e., bird bending, which is created by abnormal stresses to which the bird is subjected during the climb and turn of the aircraft between lines. Such aerodynamic noise is usually manifested by an anomaly on the coaxial in-phase channel only, although severe stresses can affect the coplanar in-phase channels as well.

## **Magnetics**

A Geometrics 823A cesium vapour magnetometer, part of the CF-1 base station, was operated at the survey base to record diurnal variations of the earth's magnetic field. The clock of the base station was synchronized with that of the airborne system to permit subsequent removal of diurnal drift. (A GEM Systems GSM-19T proton precession magnetometer was also operated as a backup unit.)



The total magnetic field data have been presented as contours on the base map using a contour interval of 5 nT where gradients permit. The map show the magnetic properties of the rock units underlying the survey areas.

The total magnetic field data have been subjected to a processing algorithm to produce maps of the calculated vertical gradient. This procedure enhances near-surface magnetic units and suppresses regional gradients. It also provides better definition and resolution of magnetic units and displays weak magnetic features which may not be clearly evident on the total field map.

There is some evidence on the magnetic map which suggest that the survey area has been subjected to deformation and/or alteration. These structural complexities are evident on the contour map as variations in magnetic intensity, irregular patterns, and as offsets or changes in strike direction. Some of the more prominent linear features are also evident on the topographic base maps.

If a specific magnetic intensity can be assigned to the rock type which is believed to host the target mineralization, it may be possible to select areas of higher priority on the basis of the total field magnetic data. This is based on the assumption that the magnetite content of the host rocks will give rise to a limited range of contour values which will permit differentiation of various lithological units.

The magnetic results, in conjunction with the other geophysical parameters, have provided valuable information which can be used to effectively map the geology and structure in the survey areas.

### **Apparent Resistivity**

Apparent resistivity maps, which display the conductive properties of the survey area, were produced from the 900 Hz and 7200 Hz coplanar data. The maximum resistivity values, which are calculated for each frequency, are 1,000 and 8,000 ohm-m respectively. These cutoffs eliminate the erratic higher resistivities which would result from unstable ratios of very small EM amplitudes.

In general, the resistivity patterns show moderately good agreement with the magnetic trends. This suggests that many of the resistivity lows and highs are probably related to bedrock features, rather than conductive overburden. There are some areas, however, where contour patterns appear to be partially influenced by topography.

There are other resistivity lows in the area. Some of these are quite extensive and could reflect "formational" conductors which may be of minor interest as direct exploration targets.

However, attention may be focused on areas where these zones appear to be faulted or folded, or where anomaly characteristics differ along strike.

## **Electromagnetic Anomalies**

The EM anomalies resulting from this survey appear to fall within one of three general categories. The first type consists of discrete, well-defined anomalies which yield marked inflections on the difference channels. These anomalies are usually attributed to conductive sulphides or graphite and are generally given a "B", "T" or "D" interpretive symbol, denoting a bedrock source.

The second class of anomalies comprises moderately broad responses which exhibit the characteristics of a half-space and do not yield well-defined inflections on the difference channels. Anomalies in this category are usually given an "S" or "H" interpretive symbol. The lack of a difference channel response usually implies a broad or flat-lying conductive source such as overburden. Some of these broad anomalies may reflect conductive rock units.

The effects of conductive overburden are evident in some of the survey areas. Although the difference channels (DIF1 and DIFQ) are extremely valuable in detecting bedrock conductors which are partially masked by conductive overburden, sharp undulations in the bedrock/overburden interface can yield anomalies in the difference channels which may be interpreted as possible bedrock conductors. Such anomalies usually fall into the "S?" or "B?" classification but may also be given an "E" interpretive symbol, denoting a resistivity contrast at the edge of a conductive unit.

The "?" symbol does not question the validity of an anomaly, but instead indicates some degree of uncertainty as to which is the most appropriate EM source model. This ambiguity results from the combination of effects from two or more conductive sources, such as overburden and bedrock, gradational changes, or moderately shallow dips. The presence of a conductive upper layer has a tendency to mask or alter the characteristics of bedrock conductors, making interpretation difficult. This problem is further exacerbated in the presence of magnetite.

The third anomaly category includes responses which are associated with magnetite. Magnetite can cause suppression or polarity reversals of the in-phase components, particularly at the lower frequencies in resistive areas. The effects of magnetite-rich rock units are evident on the multi-parameter geophysical data profiles, as negative excursions of the 900 Hz in-phase channels.

In areas where EM responses are evident primarily on the quadrature components, zones of poor conductivity are indicated. Where these responses are coincident with magnetic anomalies, it is possible that the in-phase component amplitudes have been suppressed by the effects of magnetite. Most of these poorly-conductive magnetic features give rise to resistivity anomalies which are only slightly below background. If it is expected that poorly-conductive economic mineralization may be associated with magnetite-rich units, most of these weakly anomalous features will be of interest. In areas where magnetite causes the in-phase components to become negative, the apparent conductance and depth of EM

anomalies will be unreliable. Magnetite effects usually give rise to overstated (higher) resistivity values and understated (shallow) depth calculations.

As economic mineralization within the area may be associated with massive to weakly disseminated sulphides, which may or may not be hosted by magnetite-rich rocks, it is impractical to assess the relative merits of EM anomalies on the basis of conductance. It is recommended that an attempt be made to compile a suite of geophysical "signatures" over any known areas of interest. Anomaly characteristics are clearly defined on the computer-processed geophysical data profiles which are supplied as one of the survey products.

A complete assessment and evaluation of the survey data should be carried out by one or more qualified professionals who have access to, and can provide a meaningful compilation of, all available geophysical, geological and geochemical data.

### **Conductors in the Survey Area**

The electromagnetic anomaly maps show the anomaly locations with the interpreted conductor type, dip, conductance and depth being indicated by symbols. Direct magnetic correlation is also shown if it exists. The strike direction and length of the conductors are indicated where anomalies can be correlated from line to line with a reasonable degree of confidence.

In areas where several conductors or conductive trends appear to be related to a common geological unit, these have been outlined as "zones" on the EM anomaly maps. The zone outlines approximate the limits of conductive units defined by the resistivity contours.

### Tanner Block

The magnetic relief varies from a low of 58085nT to a high of 58109nT on the Tanner Block. Generally there is low magnetic relief in the survey area as the dynamic range is only 24nT.

The weakly magnetic Tanner Block, which yields a range of only 24 nT, is intersected by a well-defined, linear magnetic low, that strikes 122° from the northwest corner of the property. Most of the bedrock conductors in this block are contained within zone 3A, a multi-conductor unit that correlates with the magnetic low.

All of the conductive sources comprising this zone are non-magnetic, so graphite is considered to be the most likely causative source. However, the possibility of non-magnetic sulphides cannot be ruled out, particularly if there are gossans in the immediate vicinity. It is recommended that this interesting conductive zone be subjected to further investigation, in order to determine its causative source. The apparent depth to the top of this zone is close to surface, usually between 0 and 15 metres.

The most conductive portion at depth is near 30130C, but there is a very weak potassium high near 30120B. At least four separate conductors are evident in this conductive zone on line 30110.

In addition to zone 3A, there are at least three other shorter conductors that may be of interest. These include conductor 30040A-30080A, a thin, near-vertical to north-dipping source, that is open to the southeast. A shorter, parallel, thin source is evident about 300 m to the north, from 30060 to 30070B. This conductor appears to be overturned, as anomaly 30060B indicates a north dip, while 30070B suggests a probable dip to the south. A weak magnetic high is centered on line 30050, between these two conductors.

Conductor 30150G-30160E is located about 600 m northeast of zone 3A. This short, thin source is situated on the eastern edge of a small, well-defined magnetic low, that could represent a non-magnetic intrusion or an alteration zone.

In addition to the foregoing, there are several short, single-line EM responses that reflect bedrock sources. Anomalies 30010A, 30010B, 30020D, 30070D,E,F and K, 30090E, 30110A and 30110B are also considered to be potential targets.

## **5. CONCLUSIONS AND RECOMMENDATIONS**

This report provides a very brief description of the survey results and describes the equipment, procedures and logistics of the survey over the Tanner block in the Nadaleen River area, Yukon Territory.

There are numerous anomalies in the survey block which are typical of graphitic or massive sulphide responses. The survey was also successful in locating a few moderately weak or broad conductors which may warrant additional work. The various maps included with this report display the magnetic, radiometric and conductive properties of the survey area. It is recommended that the survey results be reviewed in detail, in conjunction with all available geophysical, geological and geochemical information. Particular reference should be made to the computer generated data profiles which clearly define the characteristics of the individual anomalies.

Most anomalies in the area are moderately strong and well-defined. The highly conductive, non-magnetic characteristics suggest that many may be due to graphitic sources. Some have been attributed to conductive overburden or deep weathering, although a few appear to be associated with magnetite-rich rock units. Others coincide with magnetic gradients which may reflect contacts, faults or shears. Such structural breaks are considered to be of particular interest as they may have influenced mineral deposition within the survey areas.



The interpreted bedrock conductors defined by the survey should be subjected to further investigation, using appropriate surface exploration techniques. Anomalies which are currently considered to be of moderately low priority may require upgrading if follow-up results are favourable, or if they occur in areas of favourable geology or geochemical anomalies.

It is also recommended that image processing of existing geophysical data be considered, in order to extract the maximum amount of information from the survey results. Current software and imaging techniques often provide valuable information on structure and lithology, which may not be clearly evident on the contour and colour maps. These techniques can yield images which define subtle, but significant, structural details.

Respectfully submitted,

**FUGRO AIRBORNE SURVEYS CORP.**

Paul A. Smith  
Geophysicist

PAS/sdp

R2058SEP.01

## APPENDIX A

### LIST OF PERSONNEL

The following personnel were involved in the acquisition, processing, interpretation and presentation of data, relating to a DIGHEM<sup>V</sup> airborne geophysical survey carried out for Manson Creek Resources Ltd., Nadaleen River area, Yukon Territory.

David Miles	Manager, Helicopter Operations/Operator
Emily Farquhar	Manager, Data Processing and Interpretation
Duane Griffith	Field Geophysicist
Luke Kukovica	Pilot (Questral Helicopters Ltd.)
Gordon Smith	Data Processing Supervisor
Elizabeth Bowslaugh	Computer Processor
Paul A. Smith	Interpretation Geophysicist
Lyn Vanderstarren	Drafting Supervisor
Susan Pothiah	Word Processing Operator
Albina Tonello	Secretary/Expeditor

The survey consisted of 57 km of coverage, flown on July 16, 2001.

All personnel are employees of Fugro Airborne Surveys, except for the pilot who is an employee of Questral Helicopters Ltd.

**APPENDIX B**  
**STATEMENT OF COST**

Date: September 5, 2001

**IN ACCOUNT WITH FUGRO AIRBORNE SURVEYS**

To: Fugro flying of Agreement dated June 7, 2001, pertaining to an Airborne Geophysical Survey in the Nadaleen River area, Yukon Territory.

Survey Charges

57 km of flying at a fixed rate of \$134.53.00/line-km  
including mobilization costs

\$7668.16

Allocation of Costs

- Data Acquisition	(80%)
- Data Processing	(10%)
- Interpretation, Report and Maps	(10%)

## BACKGROUND INFORMATION

### Electromagnetics

DIGHEM electromagnetic responses fall into two general classes, discrete and broad. The discrete class consists of sharp, well-defined anomalies from discrete conductors such as sulphide lenses and steeply dipping sheets of graphite and sulphides. The broad class consists of wide anomalies from conductors having a large horizontal surface such as flatly dipping graphite or sulphide sheets, saline water-saturated sedimentary formations, conductive overburden and rock, and geothermal zones. A vertical conductive slab with a width of 200 m would straddle these two classes.

The vertical sheet (half plane) is the most common model used for the analysis of discrete conductors. All anomalies plotted on the geophysical maps are analyzed according to this model. The following section entitled **Discrete Conductor Analysis** describes this model in detail, including the effect of using it on anomalies caused by broad conductors such as conductive overburden.

The conductive earth (half-space) model is suitable for broad conductors. Resistivity contour maps result from the use of this model. A later section entitled **Resistivity Mapping** describes the method further, including the effect of using it on anomalies caused by discrete conductors such as sulphide bodies.

## **Geometric Interpretation**

The geophysical interpreter attempts to determine the geometric shape and dip of the conductor. Figure C-1 shows typical DIGHEM anomaly shapes which are used to guide the geometric interpretation.

## **Discrete Conductor Analysis**

The EM anomalies appearing on the electromagnetic map are analyzed by computer to give the conductance (i.e., conductivity-thickness product) in siemens (mhos) of a vertical sheet model. This is done regardless of the interpreted geometric shape of the conductor. This is not an unreasonable procedure, because the computed conductance increases as the electrical quality of the conductor increases, regardless of its true shape. DIGHEM anomalies are divided into seven grades of conductance, as shown in Table C-1. The conductance in siemens (mhos) is the reciprocal of resistance in ohms.

The conductance value is a geological parameter because it is a characteristic of the conductor alone. It generally is independent of frequency, flying height or depth of burial, apart from the averaging over a greater portion of the conductor as height increases. Small anomalies from deeply buried strong conductors are not confused with small anomalies from shallow weak conductors because the former will have larger conductance values.

**Table C-1. EM Anomaly Grades**

Anomaly Grade	Siemens
7	> 100
6	50 - 100
5	20 - 50
4	10 - 20
3	5 - 10
2	1 - 5
1	< 1

Conductive overburden generally produces broad EM responses which may not be shown as anomalies on the geophysical maps. However, patchy conductive overburden in otherwise resistive areas can yield discrete anomalies with a conductance grade (cf. Table C-1) of 1, 2 or even 3 for conducting clays which have resistivities as low as 50 ohm-m. In areas where ground resistivities are below 10 ohm-m, anomalies caused by weathering variations and similar causes can have any conductance grade. The anomaly shapes from the multiple coils often allow such conductors to be recognized, and these are indicated by the letters S, H, and sometimes E on the geophysical maps (see EM legend on maps).

For bedrock conductors, the higher anomaly grades indicate increasingly higher conductances. Examples: DIGHEM's New Inco copper discovery (Noranda, Canada) yielded a grade 5 anomaly, as did the neighbouring copper-zinc Magusi River ore body; Mattabi (copper-zinc, Sturgeon Lake, Canada) and Whistle (nickel, Sudbury, Canada) gave grade 6; and DIGHEM's Montcalm nickel-copper discovery (Timmins, Canada) yielded a grade 7 anomaly. Graphite and sulphides can span all grades but, in any particular survey area, field work may show that the different grades indicate different types of conductors.

- Appendix C.4 -

Strong conductors (i.e., grades 6 and 7) are characteristic of massive sulphides or graphite.

Moderate conductors (grades 4 and 5) typically reflect graphite or sulphides of a less massive character, while weak bedrock conductors (grades 1 to 3) can signify poorly connected graphite or heavily disseminated sulphides. Grades 1 and 2 conductors may not respond to ground EM equipment using frequencies less than 2000 Hz.

The presence of sphalerite or gangue can result in ore deposits having weak to moderate conductances. As an example, the three million ton lead-zinc deposit of Restigouche Mining Corporation near Bathurst, Canada, yielded a well-defined grade 2 conductor. The 10 percent by volume of sphalerite occurs as a coating around the fine grained massive pyrite, thereby inhibiting electrical conduction. Faults, fractures and shear zones may produce anomalies which typically have low conductances (e.g., grades 1 to 3). Conductive rock formations can yield anomalies of any conductance grade. The conductive materials in such rock formations can be salt water, weathered products such as clays, original depositional clays, and carbonaceous material.

For each interpreted electromagnetic anomaly on the geophysical maps, a letter identifier and an interpretive symbol are plotted beside the EM grade symbol. The horizontal rows of dots, under the interpretive symbol, indicate the anomaly amplitude on the flight record. The vertical column of dots, under the anomaly letter, gives the estimated depth. In areas where anomalies are crowded, the letter identifiers, interpretive symbols and dots may be obliterated. The EM grade symbols, however, will always be discernible, and the obliterated information can be obtained from the anomaly listing appended to this report.

- Appendix C.5 -

The purpose of indicating the anomaly amplitude by dots is to provide an estimate of the reliability of the conductance calculation. Thus, a conductance value obtained from a large ppm anomaly (3 or 4 dots) will tend to be accurate whereas one obtained from a small ppm anomaly (no dots) could be quite inaccurate. The absence of amplitude dots indicates that the anomaly from the coaxial coil-pair is 5 ppm or less on both the in-phase and quadrature channels. Such small anomalies could reflect a weak conductor at the surface or a stronger conductor at depth. The conductance grade and depth estimate illustrates which of these possibilities fits the recorded data best.

The conductance measurement is considered more reliable than the depth estimate. There are a number of factors which can produce an error in the depth estimate, including the averaging of topographic variations by the altimeter, overlying conductive overburden, and the location and attitude of the conductor relative to the flight line. Conductor location and attitude can provide an erroneous depth estimate because the stronger part of the conductor may be deeper or to one side of the flight line, or because it has a shallow dip. A heavy tree cover can also produce errors in depth estimates. This is because the depth estimate is computed as the distance of bird from conductor, minus the altimeter reading. The altimeter can lock onto the top of a dense forest canopy. This situation yields an erroneously large depth estimate but does not affect the conductance estimate.

Dip symbols are used to indicate the direction of dip of conductors. These symbols are used only when the anomaly shapes are unambiguous, which usually requires a fairly resistive environment.

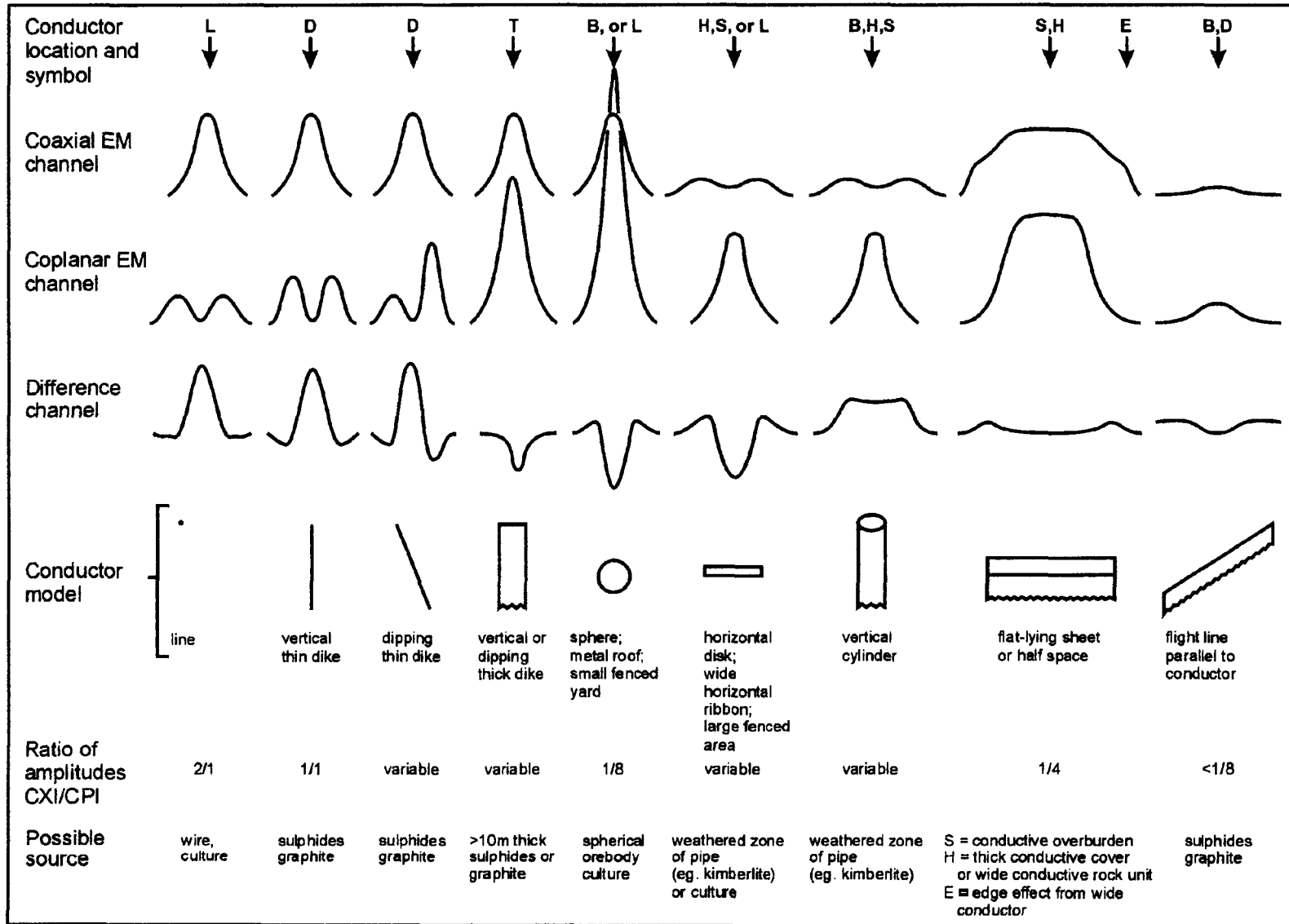


- Appendix C.6 -

A further interpretation is presented on the EM map by means of the line-to-line correlation of bedrock anomalies, which is based on a comparison of anomaly shapes on adjacent lines. This provides conductor axes which may define the geological structure over portions of the survey area. The absence of conductor axes in an area implies that anomalies could not be correlated from line to line with reasonable confidence.

DIGHEM electromagnetic anomalies are designed to provide a correct impression of conductor quality by means of the conductance grade symbols. The symbols can stand alone with geology when planning a follow-up program. The actual conductance values are printed in the attached anomaly list for those who wish quantitative data. The anomaly ppm and depth are indicated by inconspicuous dots which should not distract from the conductor patterns, while being helpful to those who wish this information. The map provides an interpretation of conductors in terms of length, strike and dip, geometric shape, conductance, depth, and thickness. The accuracy is comparable to an interpretation from a high quality ground EM survey having the same line spacing.

- Appendix C.7 -



Typical DIGHEM anomaly shapes  
Figure C-1

- Appendix C.8 -

The attached EM anomaly list provides a tabulation of anomalies in ppm, conductance, and depth for the vertical sheet model. The EM anomaly list also shows the conductance and depth for a thin horizontal sheet (whole plane) model, but only the vertical sheet parameters appear on the EM map. The horizontal sheet model is suitable for a flatly dipping thin bedrock conductor such as a sulphide sheet having a thickness less than 10 m. The list also shows the resistivity and depth for a conductive earth (half-space) model, which is suitable for thicker slabs such as thick conductive overburden. In the EM anomaly list, a depth value of zero for the conductive earth model, in an area of thick cover, warns that the anomaly may be caused by conductive overburden.

Since discrete bodies normally are the targets of EM surveys, local base (or zero) levels are used to compute local anomaly amplitudes. This contrasts with the use of true zero levels which are used to compute true EM amplitudes. Local anomaly amplitudes are shown in the EM anomaly list and these are used to compute the vertical sheet parameters of conductance and depth. Not shown in the EM anomaly list are the true amplitudes which are used to compute the horizontal sheet and conductive earth parameters.

### **Questionable Anomalies**

DIGHEM maps may contain EM responses which are displayed as asterisks (\*). These responses denote weak anomalies of indeterminate conductance, which may reflect one of the following: a weak conductor near the surface, a strong conductor at depth (e.g., 100 to 120 m below surface) or to one side of the flight line, or aerodynamic noise. Those

responses which have the appearance of valid bedrock anomalies on the flight profiles are indicated by appropriate interpretive symbols (see EM legend on maps). The others probably do not warrant further investigation unless their locations are of considerable geological interest.

### **The Thickness Parameter**

DIGHEM can provide an indication of the thickness of a steeply dipping conductor. The amplitude of the coplanar anomaly (e.g., CPI channel on the digital profile) increases relative to the coaxial anomaly (e.g., CXI) as the apparent thickness increases, i.e., the thickness in the horizontal plane. (The thickness is equal to the conductor width if the conductor dips at 90 degrees and strikes at right angles to the flight line.) This report refers to a conductor as thin when the thickness is likely to be less than 3 m, and thick when in excess of 10 m. Thick conductors are indicated on the EM map by parentheses "( )". For base metal exploration in steeply dipping geology, thick conductors can be high priority targets because many massive sulphide ore bodies are thick, whereas non-economic bedrock conductors are often thin. The system cannot sense the thickness when the strike of the conductor is subparallel to the flight line, when the conductor has a shallow dip, when the anomaly amplitudes are small, or when the resistivity of the environment is below 100 ohm-m.

## **Resistivity Mapping**

Resistivity mapping is useful in areas where broad or flat lying conductive units are of interest. One example of this is the clay alteration which is associated with Carlin-type deposits in the south west United States. The Dighem system was able to identify the clay alteration zone over the Cove deposit. The alteration zone appeared as a strong resistivity low on the 900 Hz resistivity parameter. The 7,200 Hz and 56,000 Hz resistivities show more of the detail in the covering sediments, and delineate a range front fault. This is typical in many areas of the south west United States, where conductive near surface sediments, which may sometimes be alkalic, attenuate the higher frequencies.

Resistivity mapping has proven successful for locating diatremes in diamond exploration. Weathering products from relatively soft kimberlite pipes produce a resistivity contrast with the unaltered host rock. In many cases weathered kimberlite pipes were associated with thick conductive layers which contrasted with overlying or adjacent relatively thin layers of lake bottom sediments or overburden.

Areas of widespread conductivity are commonly encountered during surveys. These conductive zones may reflect alteration zones, shallow-dipping sulphide or graphite-rich units or conductive overburden. In such areas, anomalies can be generated by decreases of only 5 m in survey altitude as well as by increases in conductivity. The typical flight record in conductive areas is characterized by in-phase and quadrature channels which are continuously active. Local EM peaks reflect either increases in conductivity of the earth or



- Appendix C.11 -

decreases in survey altitude. For such conductive areas, apparent resistivity profiles and contour maps are necessary for the correct interpretation of the airborne data. The advantage of the resistivity parameter is that anomalies caused by altitude changes are virtually eliminated, so the resistivity data reflect only those anomalies caused by conductivity changes. The resistivity analysis also helps the interpreter to differentiate between conductive bedrock and conductive overburden. For example, discrete conductors will generally appear as narrow lows on the contour map and broad conductors (e.g., overburden) will appear as wide lows.

The apparent resistivity is calculated using the pseudo-layer (or buried) half-space model defined by Fraser (1978)<sup>6</sup>. This model consists of a resistive layer overlying a conductive half-space. The depth channels give the apparent depth below surface of the conductive material. The apparent depth is simply the apparent thickness of the overlying resistive layer. The apparent depth (or thickness) parameter will be positive when the upper layer is more resistive than the underlying material, in which case the apparent depth may be quite close to the true depth.

The apparent depth will be negative when the upper layer is more conductive than the underlying material, and will be zero when a homogeneous half-space exists. The apparent depth parameter must be interpreted cautiously because it will contain any errors which may exist in the measured altitude of the EM bird (e.g., as caused by a dense tree

---

<sup>6</sup> Resistivity mapping with an airborne multicoil electromagnetic system: *Geophysics*, v.43, p.144-172.

cover). The inputs to the resistivity algorithm are the in-phase and quadrature components of the coplanar coil-pair. The outputs are the apparent resistivity of the conductive half-space (the source) and the sensor-source distance. The flying height is not an input variable, and the output resistivity and sensor-source distance are independent of the flying height when the conductivity of the measured material is sufficient to yield significant in-phase as well as quadrature responses. The apparent depth, discussed above, is simply the sensor-source distance minus the measured altitude or flying height. Consequently, errors in the measured altitude will affect the apparent depth parameter but not the apparent resistivity parameter.

The apparent depth parameter is a useful indicator of simple layering in areas lacking a heavy tree cover. The DIGHEM system has been flown for purposes of permafrost mapping, where positive apparent depths were used as a measure of permafrost thickness. However, little quantitative use has been made of negative apparent depths because the absolute value of the negative depth is not a measure of the thickness of the conductive upper layer and, therefore, is not meaningful physically. Qualitatively, a negative apparent depth estimate usually shows that the EM anomaly is caused by conductive overburden. Consequently, the apparent depth channel can be of significant help in distinguishing between overburden and bedrock conductors.

## **Interpretation in Conductive Environments**

Environments having low background resistivities (e.g., below 30 ohm-m for a 900 Hz system) yield very large responses from the conductive ground. This usually prohibits the recognition of discrete bedrock conductors. However, DIGHEM data processing techniques produce three parameters which contribute significantly to the recognition of bedrock conductors in conductive environments. These are the in-phase and quadrature difference channels (DIFI and DIFQ, which are available only on systems with common frequencies on orthogonal coil pairs), and the resistivity and depth channels (RES and DP) for each coplanar frequency.

The EM difference channels (DIFI and DIFQ) eliminate most of the responses from conductive ground, leaving responses from bedrock conductors, cultural features (e.g., telephone lines, fences, etc.) and edge effects. Edge effects often occur near the perimeter of broad conductive zones. This can be a source of geologic noise. While edge effects yield anomalies on the EM difference channels, they do not produce resistivity anomalies. Consequently, the resistivity channel aids in eliminating anomalies due to edge effects. On the other hand, resistivity anomalies will coincide with the most highly conductive sections of conductive ground, and this is another source of geologic noise. The recognition of a bedrock conductor in a conductive environment therefore is based on the anomalous responses of the two difference channels (DIFI and DIFQ) and the resistivity channels (RES). The most favourable situation is where anomalies coincide on all channels.

The DP channels, which give the apparent depth to the conductive material, also help to determine whether a conductive response arises from surficial material or from a conductive zone in the bedrock. When these channels ride above the zero level on the digital profiles (i.e., depth is negative), it implies that the EM and resistivity profiles are responding primarily to a conductive upper layer, i.e., conductive overburden. If the DP channels are below the zero level, it indicates that a resistive upper layer exists, and this usually implies the existence of a bedrock conductor. If the low frequency DP channel is below the zero level and the high frequency DP is above, this suggests that a bedrock conductor occurs beneath conductive cover.

## **Reduction of Geologic Noise**

Geologic noise refers to unwanted geophysical responses. For purposes of airborne EM surveying, geologic noise refers to EM responses caused by conductive overburden and magnetic permeability. It was mentioned previously that the EM difference channels (i.e., channel DIFI for in-phase and DIFQ for quadrature) tend to eliminate the response of conductive overburden.

Magnetite produces a form of geological noise on the in-phase channels of all EM systems.

Rocks containing less than 1% magnetite can yield negative in-phase anomalies caused by magnetic permeability. When magnetite is widely distributed throughout a survey area, the in-phase EM channels may continuously rise and fall, reflecting variations in the magnetite percentage, flying height, and overburden thickness. This can lead to difficulties in

recognizing deeply buried bedrock conductors, particularly if conductive overburden also exists. However, the response of broadly distributed magnetite generally vanishes on the in-phase difference channel DIFI. This feature can be a significant aid in the recognition of conductors which occur in rocks containing accessory magnetite.

### **EM Magnetite Mapping**

The information content of DIGHEM data consists of a combination of conductive eddy current responses and magnetic permeability responses. The secondary field resulting from conductive eddy current flow is frequency-dependent and consists of both in-phase and quadrature components, which are positive in sign. On the other hand, the secondary field resulting from magnetic permeability is independent of frequency and consists of only an in-phase component which is negative in sign. When magnetic permeability manifests itself by decreasing the measured amount of positive in-phase, its presence may be difficult to recognize. However, when it manifests itself by yielding a negative in-phase anomaly (e.g., in the absence of eddy current flow), its presence is assured. In this latter case, the negative component can be used to estimate the percent magnetite content.

A magnetite mapping technique was developed for the coplanar coil-pair of DIGHEM. The method can be complementary to magnetometer mapping in certain cases. Compared to magnetometry, it is far less sensitive but is more able to resolve closely spaced magnetite zones, as well as providing an estimate of the amount of magnetite in the rock. The method is sensitive to 1/4% magnetite by weight when the EM sensor is at a height of 30 m above a

magnetitic half-space. It can individually resolve steep dipping narrow magnetite-rich bands which are separated by 60 m. Unlike magnetometry, the EM magnetite method is unaffected by remanent magnetism or magnetic latitude.

The EM magnetite mapping technique provides estimates of magnetite content which are usually correct within a factor of 2 when the magnetite is fairly uniformly distributed. EM magnetite maps can be generated when magnetic permeability is evident as negative in-phase responses on the data profiles.

Like magnetometry, the EM magnetite method maps only bedrock features, provided that the overburden is characterized by a general lack of magnetite. This contrasts with resistivity mapping which portrays the combined effect of bedrock and overburden.

## **Recognition of Culture**

Cultural responses include all EM anomalies caused by man-made metallic objects. Such anomalies may be caused by inductive coupling or current gathering. The concern of the interpreter is to recognize when an EM response is due to culture. Points of consideration used by the interpreter, when coaxial and coplanar coil-pairs are operated at a common frequency, are as follows:

1. Channels CXP and CPP monitor 60 Hz radiation. An anomaly on these channels shows that the conductor is radiating power. Such an indication is normally a



guarantee that the conductor is cultural. However, care must be taken to ensure that the conductor is not a geologic body which strikes across a power line, carrying leakage currents.

2. A flight which crosses a "line" (e.g., fence, telephone line, etc.) yields a centre-peaked coaxial anomaly and an m-shaped coplanar anomaly<sup>7</sup>. When the flight crosses the cultural line at a high angle of intersection, the amplitude ratio of coaxial/coplanar response is 8. Such an EM anomaly can only be caused by a line. The geologic body which yields anomalies most closely resembling a line is the vertically dipping thin dike. Such a body, however, yields an amplitude ratio of 4 rather than 8. Consequently, an m-shaped coplanar anomaly with a CXI/CPI amplitude ratio of 8 is virtually a guarantee that the source is a cultural line.
3. A flight which crosses a sphere or horizontal disk yields centre-peaked coaxial and coplanar anomalies with a CXI/CPI amplitude ratio (i.e., coaxial/coplanar) of 1/8. In the absence of geologic bodies of this geometry, the most likely conductor is a metal roof or small fenced yard<sup>8</sup>. Anomalies of this type are virtually certain to be cultural if they occur in an area of culture.

---

<sup>7</sup> See Figure C-1 presented earlier.

<sup>8</sup> It is a characteristic of EM that geometrically similar anomalies are obtained from: (1) a planar conductor, and (2) a wire which forms a loop having dimensions identical to the perimeter of the equivalent planar conductor.

4. A flight which crosses a horizontal rectangular body or wide ribbon yields an m-shaped coaxial anomaly and a centre-peaked coplanar anomaly. In the absence of geologic bodies of this geometry, the most likely conductor is a large fenced area.<sup>5</sup> Anomalies of this type are virtually certain to be cultural if they occur in an area of culture.
  
5. EM anomalies which coincide with culture, as seen on the camera film or video display, are usually caused by culture. However, care is taken with such coincidences because a geologic conductor could occur beneath a fence, for example. In this example, the fence would be expected to yield an m-shaped coplanar anomaly as in case #2 above. If, instead, a centre-peaked coplanar anomaly occurred, there would be concern that a thick geologic conductor coincided with the cultural line.
  
6. The above description of anomaly shapes is valid when the culture is not conductively coupled to the environment. In this case, the anomalies arise from inductive coupling to the EM transmitter. However, when the environment is quite conductive (e.g., less than 100 ohm-m at 900 Hz), the cultural conductor may be conductively coupled to the environment. In this latter case, the anomaly shapes tend to be governed by current gathering. Current gathering can completely distort the anomaly shapes, thereby complicating the identification of cultural anomalies. In such circumstances, the interpreter can only rely on the radiation channels and on the camera film or video records.

## **Magnetics**

Total field magnetics provides information on the magnetic properties of the earth materials in the survey area. The information can be used to locate magnetic bodies of direct interest for exploration, and for structural and lithological mapping.

The total field magnetic response reflects the abundance of magnetic material, in the source. Magnetite is the most common magnetic mineral. Other minerals such as ilmenite, pyrrhotite, franklinite, chromite, hematite, arsenopyrite, limonite and pyrite are also magnetic, but to a lesser extent than magnetite on average.

In some geological environments, an EM anomaly with magnetic correlation has a greater likelihood of being produced by sulphides than one which is non-magnetic. However, sulphide ore bodies may be non-magnetic (e.g., the Kidd Creek deposit near Timmins, Canada) as well as magnetic (e.g., the Mattabi deposit near Sturgeon Lake, Canada).

Iron ore deposits will be anomalously magnetic in comparison to surrounding rock due to the concentration of iron minerals such as magnetite, ilmenite and hematite.

Changes in magnetic susceptibility often allow rock units to be differentiated based on the total field magnetic response. Geophysical classifications may differ from geological classifications if various magnetite levels exist within one general geological classification.

- Appendix C.20 -

Geometric considerations of the source such as shape, dip and depth, inclination of the earth's field and remanent magnetization will complicate such an analysis.

In general, mafic lithologies contain more magnetite and are therefore more magnetic than many sediments which tend to be weakly magnetic. Metamorphism and alteration can also increase or decrease the magnetization of a rock unit.

Textural differences on a total field magnetic contour, colour or shadow map due to the frequency of activity of the magnetic parameter resulting from inhomogeneities in the distribution of magnetite within the rock, may define certain lithologies. For example, near surface volcanics may display highly complex contour patterns with little line-to-line correlation.

Rock units may be differentiated based on the plan shapes of their total field magnetic responses. Mafic intrusive plugs can appear as isolated "bulls-eye" anomalies. Granitic intrusives appear as sub-circular zones, and may have contrasting rings due to contact metamorphism. Generally, granitic terrain will lack a pronounced strike direction, although granite gneiss may display strike.

Linear north-south units are theoretically not well-defined on total field magnetic maps in equatorial regions due to the low inclination of the earth's magnetic field. However, most stratigraphic units will have variations in composition along strike which will cause the units to appear as a series of alternating magnetic highs and lows.

- Appendix C.21 -

Faults and shear zones may be characterized by alteration which causes destruction of magnetite (e.g., weathering) which produces a contrast with surrounding rock. Structural breaks may be filled by magnetite-rich, fracture filling material as is the case with diabase dikes, or by non-magnetic felsic material.

Faulting can also be identified by patterns in the magnetic total field contours or colours. Faults and dikes tend to appear as lineaments and often have strike lengths of several kilometres. Offsets in narrow, magnetic, stratigraphic trends also delineate structure. Sharp contrasts in magnetic lithologies may arise due to large displacements along strike-slip or dip-slip faults.

### **Radiometrics**

Radioelement concentrations are measures of the abundance of radioactive elements in the rock. The original abundance of the radioelements in any rock can be altered by the subsequent processes of metamorphism and weathering.

Gamma radiation in the range which is measured in the thorium, potassium, uranium and total count windows is strongly attenuated by rock, overburden and water. Almost all of the total radiation measured from rock and overburden originates in the upper .5 metres. Moisture in soil and bodies of water will mask the radioactivity from underlying rock. Weathered rock materials which have been displaced by glacial, water or wind action will not reflect the general composition of the underlying bedrock. Where residual soils exist,

- Appendix C.22 -

they may reflect the composition of underlying rock except where equilibrium does not exist between the original radioelement and the products in its decay series.

Radioelement counts (expressed as counts per second) are the rates of detection of the gamma radiation from specific decaying particles corresponding to products in each radioelements decay series. The radiation source for uranium is bismuth (Bi-214), for thorium it is thallium (Tl-208) and for potassium it is potassium (K-40).

The uranium and thorium radioelement concentrations are dependent on a state of equilibrium between the parent and daughter products in the decay series. Some daughter products in the uranium decay are long lived and could be removed by processes such as leaching. One product in the series, radon (Rn-222), is a gas which can easily escape. Both of these factors can affect the degree to which the calculated uranium concentrations reflect the actual composition of the source rock. Because the daughter products of thorium are relatively short lived, there is more likelihood that the thorium decay series is in equilibrium.

Lithological discrimination can be based on the measured relative concentrations and total, combined, radioactivity of the radioelements. Feldspar and mica contain potassium. Zircon, sphene and apatite are accessory minerals in igneous rocks which are sources of uranium and thorium. Monazite, thorianite, thorite, uraninite and uranothorite are also sources of uranium and thorium which are found in granites and pegmatites.



- Appendix C.23 -

In general, the abundance of uranium, thorium and potassium in igneous rock increases with acidity. Pegmatites commonly have elevated concentrations of uranium relative to thorium. Sedimentary rocks derived from igneous rocks may have characteristic signatures which are influenced by their parent rocks, but these will have been altered by subsequent weathering and alteration.

Metamorphism and alteration will cause variations in the abundance of certain radioelements relative to each other. For example, alterative processes may cause uranium enrichment to the extent that a rock will be of economic interest. Uranium anomalies are more likely to be economically significant if they consist of an increase in the uranium relative to thorium and potassium, rather than a sympathetic increase in all three radioelements.

Faults can exhibit radioactive highs due to increased permeability which allows radon migration, or as lows due to structural control of drainage and fluvial sediments which attenuate gamma radiation from the underlying rocks. Faults can also be recognized by sharp contrasts in radiometric lithologies due to large strike-slip or dip-slip displacements. Changes in relative radioelement concentrations due to alteration will also define faults.

Similar to magnetics, certain rock types can be identified by their plan shapes if they also produce a radiometric contrast with surrounding rock. For example, granite intrusions will appear as sub-circular bodies, and may display concentric zonations. They will tend to lack a prominent strike direction. Offsets of narrow, continuous, stratigraphic units with

contrasting radiometric signatures can identify faulting, and folding of stratigraphic trends will also be apparent.

**APPENDIX D**

**EM ANOMALY LIST**

EM Anomaly List

					CX 5500 HZ		CP 7200 HZ		CP 900 HZ		Vertical Dike		Mag. Corr
Label	Fid	Interp	XUTM	YUTM	Real	Quad	Real	Quad	Real	Quad	COND	DEPTH*	
			m	m	ppm	ppm	ppm	ppm	ppm	ppm	siemens	m	NT
LINE	19010		FLIGHT 4										
H	3818.3	B?	578886	7114995	2.5	24.6	61.5	154.2	75.6	26.0	---	---	0
I	3883.0	B?	579506	7114998	15.6	52.7	39.9	271.3	56.7	38.1	0.5	0	0
J	3927.4	S	580342	7115000	0.0	19.9	8.9	158.4	0.3	21.3	---	---	0

the  
or  
of a  
Nadaleen River Area A

CX = COAXIAL

CP = COPLANAR

Note:EM values shown above  
are local amplitudes

\*Estimated Depth may be unreliable because  
stronger part of the conductor may be deeper  
to one side of the flight line, or because  
shallow dip or magnetite/overburden effects

LINE	19010		FLIGHT 4													
A	3533.0	H	575118	7114989		27.3	29.9	149.5	248.4	77.6	69.9		1.6	5		0
B	3536.8	B?	575194	7114991		24.8	43.9	149.5	248.4	77.6	69.9		0.9	1		1181
C	3556.6	S?	575621	7115004		9.1	40.4	118.6	266.1	54.0	51.5		0.3	0		0
D	3597.1	S?	576510	7114997		0.1	63.6	44.0	272.6	35.8	58.6		---	---		294
E	3685.8	D	577476	7114998		89.8	105.9	267.4	423.2	94.7	87.3		2.1	0		0
F	3717.5	B?	578045	7114997		16.2	27.8	55.2	153.2	1.4	26.3		0.8	1		24
G	3765.4	S?	578465	7114997		9.6	15.9	64.7	64.7	67.3	8.9		---	---		157

the  
or  
of a  
Nadaleen River Area A

CX = COAXIAL

CP = COPLANAR

Note:EM values shown above  
are local amplitudes

- 10 -

\*Estimated Depth may be unreliable because  
stronger part of the conductor may be deeper  
to one side of the flight line, or because  
shallow dip or magnetite/overburden effects

LINE	30130		FLIGHT 4													
A	723.4	H	584502	7103626		4.4	9.5	27.7	56.0	2.6	11.9		0.4	25		0
B	699.2	H	584512	7103989		12.3	30.0	35.8	419.2	20.7	22.0		0.6	6		0
C	692.7	B	584511	7104164		266.7	85.8	1193.7	419.2	692.3	478.2		15.8	0		0
D	690.1	B	584509	7104223		99.6	0.0	1315.8	920.8	692.3	576.1		---	---		0
E	686.4	B	584504	7104293		204.9	162.0	1315.8	920.8	692.3	576.1		4.4	0		0

LINE	30140		FLIGHT 3													
A	2361.3	H	584697	7103475		23.5	27.0	61.2	74.3	5.6	24.9		1.4	9		0
B	2374.3	H	584703	7103800		8.0	31.2	416.0	112.9	159.9	19.6		0.3	0		0
C	2380.2	B	584704	7104007		86.6	37.4	416.0	163.7	159.9	174.8		7.2	0		0
D	2382.7	B	584701	7104091		95.5	39.3	416.0	173.3	159.9	174.8		8.0	0		0

LINE	30150		FLIGHT 3													
A	2274.9	S	584899	7103623		16.5	41.3	59.7	247.0	3.0	37.6		0.6	0		0
B	2270.6	B?	584897	7103708		0.1	25.0	48.7	247.0	13.3	39.9		---	---		0
C	2262.0	D	584894	7103857		111.1	13.1	882.8	532.1	317.1	371.0		51.5	3		0
D	2258.6	D	584894	7103922		211.8	122.3	882.8	532.1	317.1	371.0		6.6	0		0

the  
or  
of a  
Nadaleen River Area A

CX = COAXIAL  
CP = COPLANAR  
Note: EM values shown above  
are local amplitudes

\*Estimated Depth may be unreliable because  
stronger part of the conductor may be deeper  
to one side of the flight line, or because  
shallow dip or magnetite/overburden effects



## EM Anomaly List

					CX 5500 HZ		CP 7200 HZ		CP 900 HZ		Vertical Dike		Mag. Corr
Label	Fid	Interp	XUTM	YUTM	Real	Quad	Real	Quad	Real	Quad	COND	DEPTH*	
			m	m	ppm	ppm	ppm	ppm	ppm	ppm	siemens	m	NT
LINE 30010					FLIGHT 4								
A	3080.0	D	582098	7103931	34.7	26.8	63.1	86.3	11.6	26.4	2.5	0	0
B	2978.5	B?	582101	7105087	8.6	15.0	25.0	92.5	1.3	15.7	0.7	8	0
C	2971.7	S	582101	7105211	0.1	14.0	25.0	92.5	8.0	15.7	---	---	0
D	2960.9	D	582103	7105410	54.4	51.9	274.0	198.1	88.2	110.6	2.3	4	0
E	2957.3	B	582103	7105469	32.4	26.1	274.0	198.1	88.2	110.6	2.3	9	0
LINE 30020					FLIGHT 4								
A	2761.3	H	582303	7103492	5.6	14.0	12.8	43.5	2.3	6.8	0.4	8	0
B	2810.9	H	582290	7104114	1.9	8.3	22.1	61.9	4.8	14.3	---	---	0
C	2855.1	E	582302	7104571	19.5	31.6	277.8	298.3	17.1	90.3	0.9	8	0
D	2861.7	D	582303	7104673	76.5	115.9	312.4	520.6	17.1	111.1	1.6	0	0
E	2864.2	E	582303	7104724	42.9	74.7	312.4	520.6	10.6	111.1	1.1	0	0
F	2872.4	S	582303	7104947	15.8	36.6	61.3	157.6	0.0	18.9	0.6	0	0
G	2889.9	B	582300	7105344	124.9	93.4	597.0	406.5	142.5	245.4	4.0	0	0
H	2892.7	B	582304	7105409	124.9	90.8	597.0	406.5	142.5	245.4	4.2	0	0
LINE 30030					FLIGHT 4								
A	2641.1	S?	582497	7104199	3.7	15.5	13.7	64.8	1.8	8.3	0.2	9	0

B	2611.5	S?	582506	7104835		21.3	43.0	59.5	191.3	0.1	27.9		0.8	0		13
C	2591.3	B	582504	7105252		109.1	47.4	535.3	242.1	204.2	225.1		7.7	0		0

LINE	30040		FLIGHT 4													
A	2375.5	D	582686	7103579		9.8	17.6	13.4	50.1	1.1	10.1		0.7	10		0
B	2449.6	H	582699	7104429		15.5	24.1	62.6	99.6	7.3	26.3		0.9	10		0
C	2460.9	B?	582699	7104749		9.1	21.9	52.2	106.7	0.3	19.7		0.5	9		0
D	2471.4	B	582705	7105107		209.1	68.0	965.3	248.2	445.3	413.2		14.3	0		0
E	2474.9	B	582705	7105215		213.5	100.2	965.3	486.8	445.3	413.2		8.7	0		0
F	2478.3	E	582705	7105295		141.1	86.9	965.3	486.8	445.3	413.2		5.3	0		0

LINE	30050		FLIGHT 4													
A	2304.3	D	582900	7103450		29.7	43.3	35.3	79.2	3.3	15.4		1.2	0		0
B	2197.7	H	582906	7104548		12.8	43.5	83.4	249.3	3.1	45.7		0.4	0		0
C	2176.6	B	582905	7105081		217.6	99.1	833.8	404.2	316.7	350.5		9.1	0		0
D	2172.2	B	582904	7105179		198.4	109.1	734.8	492.3	316.7	350.5		6.9	0		0
E	2168.7	E	582906	7105254		150.4	97.7	734.8	492.3	316.7	305.7		5.1	0		0

the  
or  
of a  
Nadaleen River Area A

CX = COAXIAL  
CP = COPLANAR  
Note: EM values shown above  
are local amplitudes

\*Estimated Depth may be unreliable because  
stronger part of the conductor may be deeper  
to one side of the flight line, or because  
shallow dip or magnetite/overburden effects

## EM Anomaly List

					CX 5500 HZ	CP 7200 HZ	CP 900 HZ	Vertical Dike	Mag. Corr				
Label	Fid	Interp	XUTM	YUTM	Real	Quad	Real	Quad	Real	Quad	COND	DEPTH*	
			m	m	ppm	ppm	ppm	ppm	ppm	ppm	siemens	m	NT
LINE	30060		FLIGHT 4										
A	1960.4	B?	583101	7103358	7.9	7.6	21.9	44.8	5.3	11.7	1.2	0	0
B	1989.2	D	583100	7103809	25.1	24.8	86.6	112.0	11.1	37.6	1.7	11	0
C	2057.9	H	583093	7104594	11.9	30.2	29.6	194.0	2.4	25.0	0.5	0	0
D	2071.1	B	583104	7104963	149.4	55.8	744.3	513.9	259.0	323.1	10.6	1	0
E	2074.5	B	583107	7105077	215.8	127.4	744.3	513.9	259.0	323.1	6.5	0	0
F	2078.1	B?	583109	7105194	20.1	2.2	744.3	513.9	259.0	323.1	---	---	0
LINE	30070		FLIGHT 4										
A	1915.5	D	583306	7103405	15.1	15.0	23.6	37.2	2.0	7.1	1.4	8	0
B	1905.3	D	583302	7103670	10.8	29.3	21.5	89.5	6.9	14.5	0.5	0	0
C	1888.1	H	583300	7103972	12.1	28.1	85.6	140.8	10.1	37.6	0.6	4	0
D	1831.6	D	583305	7104385	7.0	19.8	28.6	148.8	1.4	20.2	0.4	4	0
E	1823.3	D	583303	7104437	12.2	43.8	65.5	239.1	2.6	34.0	0.4	0	0
F	1818.9	D	583303	7104492	12.6	33.3	65.5	239.1	2.6	34.0	0.5	0	0
G	1802.6	D	583302	7104799	110.1	49.0	651.8	208.7	260.3	274.2	7.5	0	0
H	1798.4	D	583300	7104913	136.2	43.3	651.8	291.9	260.3	274.2	12.8	0	0
I	1795.2	B	583300	7104997	136.4	66.6	651.8	291.9	234.1	274.2	7.1	0	0
J	1792.5	E	583302	7105070	99.6	59.5	651.8	291.9	234.1	274.2	4.9	0	0
K	1780.3	D	583301	7105437	11.9	39.4	24.0	96.7	3.3	15.9	0.4	0	0

LINE	30080		FLIGHT 4													
A	1565.6	D	583499	7103362		17.8	14.2	72.5	89.8	12.1	30.1		1.9	12		0
B	1580.6	B	583499	7103761		17.9	10.4	151.7	39.3	42.5	63.1		2.9	21		0
C	1634.8	D	583505	7104678		89.7	34.8	335.6	192.2	122.4	129.7		8.4	12		0
D	1646.4	D	583500	7104877		56.6	16.2	254.8	62.5	102.7	95.9		11.1	7		0

LINE	30090		FLIGHT 4													
A	1500.9	H	583699	7103706		15.8	13.9	78.9	66.6	15.9	31.0		1.7	16		0
B	1429.1	B?	583701	7104115		1.9	4.3	20.6	29.0	1.5	8.7		---	---		0
C	1397.3	B	583697	7104575		185.0	78.3	1179.3	434.4	515.1	474.9		9.5	0		0
D	1392.4	B	583699	7104712		303.5	118.3	1179.3	434.4	515.1	474.9		12.6	0		0
E	1352.0	D	583710	7105435		9.8	32.4	25.5	115.6	1.7	12.0		0.4	0		0

LINE	30100		FLIGHT 4													
A	1234.5	H	583904	7104341		20.5	18.3	102.2	129.8	29.8	47.1		1.8	16		0
B	1245.0	B	583899	7104463		93.8	36.9	470.2	67.9	319.8	178.3		8.4	0		0
C	1254.1	B	583899	7104536		187.8	100.0	1041.1	477.3	520.8	522.8		7.1	0		0

the  
or  
of a

CX = COAXIAL  
CP = COPLANAR

Note: EM values shown above  
are local amplitudes

Nadaleen River Area A

- 2 -

\*Estimated Depth may be unreliable because  
stronger part of the conductor may be deeper  
to one side of the flight line, or because  
shallow dip or magnetite/overburden effects

## EM Anomaly List

					CX 5500 HZ		CP 7200 HZ		CP 900 HZ		Vertical Dike		Mag. Corr
Label	Fid	Interp	XUTM	YUTM	Real	Quad	Real	Quad	Real	Quad	COND	DEPTH*	
			m	m	ppm	ppm	ppm	ppm	ppm	ppm	siemens	m	NT
LINE 30100			FLIGHT 4										
D	1262.8	D	583902	7104640	236.1	69.9	410.5	429.5	484.7	393.4	17.1	0	0
LINE 30110			FLIGHT 4										
A	1097.0	D	584097	7103423	22.9	28.0	83.1	186.6	18.4	31.5	1.3	11	0
B	1073.9	B	584099	7103707	7.2	11.7	60.7	91.1	4.2	24.2	0.7	17	0
C	1039.5	D	584109	7104288	78.3	9.9	340.2	123.8	257.1	124.8	41.2	3	0
D	1030.5	B	584105	7104448	217.6	186.1	1106.6	914.8	370.8	520.3	4.1	0	0
E	1028.4	B	584107	7104478	235.1	186.1	1106.6	914.8	370.8	520.3	4.6	0	0
F	1020.3	D	584103	7104585	140.8	89.7	1435.3	421.6	334.6	554.1	5.1	3	0
G	1015.5	E	584099	7104658	143.5	64.0	719.7	421.6	42.7	277.6	8.2	0	10
H	989.0	S?	584099	7105265	3.1	19.2	5.7	79.4	2.0	10.9	0.2	0	0
LINE 30120			FLIGHT 4										
A	849.3	H	584299	7103641	3.4	10.1	47.5	141.8	3.4	28.9	0.3	15	0
B	871.2	B	584294	7104154	136.1	13.9	620.8	224.5	364.9	229.9	68.8	0	0
C	874.9	B	584298	7104265	66.8	21.0	620.8	260.0	364.9	223.7	10.3	6	0
D	877.4	B	584299	7104337	116.9	51.8	595.3	260.0	364.9	224.9	7.7	0	0
E	920.3	S	584303	7105219	5.8	28.2	6.2	80.8	0.6	11.9	0.3	0	0
F	934.7	S	584304	7105442	4.8	45.4	8.6	183.5	1.5	24.2	0.1	0	0

## EM Anomaly List

					CX 5500 HZ	CP 7200 HZ	CP 900 HZ	Vertical Dike	Mag. Corr				
Label	Fid	Interp	XUTM	YUTM	Real	Quad	Real	Quad	Real	Quad	COND	DEPTH*	
			m	m	ppm	ppm	ppm	ppm	ppm	ppm	siemens	m	NT
LINE	30150		FLIGHT 3										
E	2256.6	B	584895	7103962	248.6	122.3	821.6	532.1	317.1	371.0	8.6	0	0
F	2235.4	S?	584901	7104407	4.7	16.9	24.2	93.2	1.7	14.9	0.3	1	0
G	2202.7	D	584894	7104820	11.4	35.5	7.9	91.1	0.1	12.3	0.4	0	0
LINE	30160		FLIGHT 3										
A	1989.3	D	585110	7103662	65.7	27.1	279.1	110.7	120.6	32.9	7.0	2	0
B	1993.1	B	585107	7103756	8.0	27.9	403.2	281.8	120.6	174.6	0.4	0	0
C	1997.4	D	585107	7103834	65.1	50.2	403.2	281.8	120.6	174.6	3.1	4	0
D	2010.2	H	585105	7104044	2.5	22.9	0.0	43.6	5.4	11.2	---	---	0
E	2043.3	B?	585097	7104719	4.9	12.8	4.9	35.2	0.0	3.9	0.4	10	0
F	2060.1	S	585097	7105064	3.2	11.8	19.8	72.6	1.0	10.9	0.3	1	0
G	2073.6	S?	585096	7105420	2.8	25.4	16.4	94.4	0.4	12.8	---	---	0
LINE	30170		FLIGHT 3										
A	1926.2	B	585302	7103610	39.8	0.7	350.7	243.4	102.5	139.8	---	---	0
B	1921.8	B	585300	7103705	42.7	34.7	350.7	243.4	102.5	139.8	2.6	4	0
C	1919.6	D	585301	7103743	64.1	46.4	350.7	243.4	102.5	139.8	3.4	0	0
D	1892.2	S	585304	7103987	2.5	8.3	9.4	92.6	2.3	11.9	---	---	0

LINE	30180		FLIGHT 3													
A	1579.1	B	585522	7103422		102.4	45.2	508.5	179.8	212.3	224.3		7.4	0		0
B	1580.8	B	585520	7103466		102.4	45.2	508.5	179.8	212.3	224.3		7.4	0		0
C	1609.0	S?	585504	7103976		5.6	15.6	20.0	90.8	0.9	6.7		0.4	7		0
D	1632.6	S	585501	7104325		7.0	27.8	21.9	123.0	1.6	20.9		0.3	0		0
E	1641.9	S	585496	7104540		6.7	21.7	22.7	53.5	1.7	10.4		0.4	0		0

LINE	30190		FLIGHT 3													
A	1534.9	D	585708	7103386		94.6	46.4	232.9	223.5	67.7	93.2		6.3	0		0
B	1513.1	S	585696	7103919		7.8	32.6	47.2	161.4	3.3	28.0		0.3	0		0
C	1369.7	S?	585698	7105367		3.9	13.3	8.8	66.3	1.5	12.0		0.3	5		0
D	1356.9	S	585697	7105521		2.3	13.8	8.8	87.1	1.2	14.3		---	---		0

LINE	39010		FLIGHT 3													
A	5136.7	B	581985	7105254		5.8	24.5	23.8	208.7	139.3	80.2		0.3	0		0
B	5101.7	E	582406	7105252		18.1	16.1	71.7	35.0	181.6	7.8		1.7	18		0
C	5091.9	D	582526	7105244		59.4	40.8	427.8	169.8	345.5	58.6		3.5	2		0
D	5083.8	B	582693	7105241		83.2	70.3	875.9	395.1	2366.2	246.1		3.0	2		0
E	5080.3	B	582774	7105242		121.4	50.5	875.9	395.1	2366.2	246.1		8.5	0		0

the  
or  
of a  
Nadaleen River Area A

CX = COAXIAL

CP = COPLANAR

Note:EM values shown above  
are local amplitudes

\*Estimated Depth may be unreliable because  
stronger part of the conductor may be deeper  
to one side of the flight line, or because  
shallow dip or magnetite/overburden effects



EM Anomaly List

					CX 5500 HZ	CP 7200 HZ	CP 900 HZ	Vertical Dike	Mag. Corr				
Label	Fid	Interp	XUTM	YUTM	Real	Quad	Real	Quad	Real	Quad	COND	DEPTH*	
			m	m	ppm	ppm	ppm	ppm	ppm	ppm	siemens	m	NT
LINE	39010		FLIGHT 3										
F	5073.8	E	582907	7105248	49.2	38.4	165.8	169.5	295.2	117.6	2.8	2	0
LINE	39020		FLIGHT 3										
A	4530.7	D	582833	7103750	19.5	27.8	42.5	66.8	67.4	39.1	1.1	0	0
B	4549.5	B?	583193	7103748	11.2	15.5	44.8	81.5	103.7	56.6	0.9	0	0
C	4565.2	S?	583461	7103749	12.3	16.0	62.7	98.1	189.0	53.6	1.0	4	0
D	4688.4	D	584119	7103752	42.7	75.2	230.1	279.1	349.9	218.5	1.1	0	0
E	4695.5	D	584221	7103753	37.9	66.8	230.1	279.1	349.9	218.5	1.1	0	0
F	4728.4	E	584954	7103752	52.2	24.8	355.0	124.7	966.3	0.0	5.4	7	0
G	4732.9	B	585066	7103756	84.0	43.2	355.0	124.7	966.3	131.7	5.7	1	0
H	4741.8	D	585212	7103755	30.6	39.6	284.5	234.8	659.9	244.8	1.4	12	0
I	4745.7	E	585291	7103750	38.8	39.6	284.5	234.8	659.9	244.8	1.9	3	0

the  
or  
of a  
Nadaleen River Area A

CX = COAXIAL  
CP = COPLANAR  
Note:EM values shown above  
are local amplitudes

\*Estimated Depth may be unreliable because  
stronger part of the conductor may be deeper  
to one side of the flight line, or because  
shallow dip or magnetite/overburden effects

**APPENDIX E**

**RADIOMETRIC PROCESSING  
CONTROL FILE**

## APPENDIX E-1

### RADIOMETRIC PROCESSING CONTROL FILE

INPUT DATABASE PARAMETER NAMES:

FID	, FID	DBASE NAME =FID
ALT	, ALTIMETER	DBASE NAME =ALTRFT
LIVE	, LIVE TIME	DBASE NAME =LIVETIME
TEMP	, TEMPERATURE (OPT.)	DBASE NAME =
BAR PRESS	, BARO PRESSURE (OPT.)	DBASE NAME =
RAW_TC	, RAW TOTAL COUNT	DBASE NAME =TCR
RAW_K	, RAW POTASSIUM	DBASE NAME =KR
RAW_U	, RAW URANIUM	DBASE NAME =UR
RAW_TH	, RAW THORIUM	DBASE NAME =THR
RAW_UP_U	, RAW URANIUM UP	DBASE NAME =URANUP
COSMIC	, RAW COSMIC TOTAL CTS	DBASE NAME =COSMIC

-----

OUTPUT DATABASE PARAMETER NAMES:

COR_TC	, COR TOTAL COUNT	DBASE NAME =TC
COR_K	, COR POTASSIUM	DBASE NAME =K
COR_U	, COR URANIUM	DBASE NAME =U
COR_TH	, COR THORIUM	DBASE NAME =TH
COR_UPU	, COR URANUP	DBASE NAME =UPU
CONC_K	, K CONCENTRATION (OPT.)	DBASE NAME =
CONC_U	, U CONCENTRATION (OPT.)	DBASE NAME =
CONC_TH	, TH CONCENTRATION (OPT.)	DBASE NAME =
EXPOSURE	, EXPOSURE RATE (OPT.)	DBASE NAME =
EXPORADR	, EXP-MR/HR(0) OR NADR-NG/HR(1)	=1

-----

TRAP NEG	, OUTPUT NEGATIVES AS ZERO (YES=1,NO=0)	=0
RAWORHG	, INPUT DATA RAW(0) OR NASVD(1)	=0

-----

HANNING FILTER LENGTH FOR EACH DATABASE PARAMETER (0=NO FILTER):

FILT_ALT	, ALTIMETER	FILTER LENGTH =5
FILT_TMP	, TEMPERATURE	FILTER LENGTH =0
FILT_PRESS	, PRESSURE	FILTER LENGTH =0
FILT_TC	, RAW TOTAL COUNT	FILTER LENGTH =0
FILT_K	, RAW POTASSIUM	FILTER LENGTH =0
FILT_U	, RAW URANIUM	FILTER LENGTH =0
FILT_TH	, RAW THORIUM	FILTER LENGTH =0
FILT_UPU	, RAW URANIUM UP	FILTER LENGTH =11
FILT_COS	, RAW COSMIC TOTAL CTS	FILTER LENGTH =0

-----

RADIOMETRIC COEFFICIENTS:

ABCK_TC	, AIRCRAFT BACKGROUND - TOTAL CTS	=86.834
ABCK_K	, AIRCRAFT BACKGROUND - POTASSIUM	=7.086
ABCK_U	, AIRCRAFT BACKGROUND - URANIUM	=3.9392
ABCK_TH	, AIRCRAFT BACKGROUND - THORIUM	=0.9282
ABCK_UPU	, AIRCRAFT BACKGROUND - URANIUM UP	=0.5210
CSR_TC	, COSMIC STRIPPING RATIO - TOTAL CTS	=0.6659
CSR_K	, COSMIC STRIPPING RATIO - POTASSIUM	=0.0392
CSR_U	, COSMIC STRIPPING RATIO - URANIUM	=0.0268
CSR_TH	, COSMIC STRIPPING RATIO - THORIUM	=0.0353
CSR_UPU	, COSMIC STRIPPING RATIO - URANIUM UP	=0.0078
RDN_ATC	, RADON - UR IN TC COEFFICIENT	=0.0
RDN_BTC	, RADON - UR IN TC CONSTANT	=0
RDN_AK	, RADON - UR IN K COEFFICIENT	=0.0
RDN_BK	, RADON - UR IN K CONSTANT	=0
RDN_ATH	, RADON - UR IN TH COEFFICIENT	=0.0

RDN_BTH	, RADON - UR IN TH CONSTANT	=0
RDN_AUPU	, RADON - UR IN UPU COEFFICIENT	=0.0
RDN_BUPU	, RADON - UR IN UPU CONSTANT	=0
RDN_A1	, RADON - U IN UPU	=0
RDN_A2	, RADON - TH IN UPU	=0.0
ALPHA	, COMPTON TH > U	=0.2480
BETA	, COMPTON TH > K	=0.3860
GAMMA	, COMPTON U > K	=0.7820
BACKA	, GRASTY BACKSCATTER U > TH (0.05)	=0.0
BACKB	, GRASTY BACKSCATTER K > TH (0.0)	=0.0
BACKG	, GRASTY BACKSCATTER K > U (0.0)	=0.0
ATN_TC	, HEIGHT ATTENUATION OF TC	=0.001628
ATN_K	, HEIGHT ATTENUATION OF K	=0.002168
ATN_U	, HEIGHT ATTENUATION OF U	=0.00972
ATN_TH	, HEIGHT ATTENUATION OF TH	=0.001987
SENS_K	, CPS PER PERCENT POTASSIUM ON GROUND	=0.0
SENS_U	, CPS PER PPM URANIUM ON GROUND	=0.0
SENS_TH	, CPS PER PPM THORIUM ON GROUND	=0.0

-----

GENERAL PARAMETERS:

S_FREQ	, RADIOMETRIC SAMPLES PER SECOND	=1
ALT_OFF	, HEIGHT OF SENSOR ABOVE ALTIMETER (ft)	=0
ALT_DTM	, SURVEY HEIGHT DATUM (ft)	=100
ALT_MAX	, MAXIMUM ALTITUDE (1000ft)	=500

-----

FLIGHT RANGES TO PROCESS, FLIGHTS TO PROCESS, FLIGHTS TO SKIP:

/ flight ranges to process  
 / specific flights to process  
 / specific flights to skip

-----

LINE RANGES TO PROCESS, LINES TO PROCESS, LINES TO SKIP:

1 999999  
 / line ranges to process  
 / specific lines to process  
 / specific lines to skip

## APPENDIX E-2

### RADIOMETRIC COEFFICIENTS

#### ALTITUDE ATTENUATION COEFFICIENT CALIBRATION

##### DATA SUMMARY :

LINE	Avg. Alt. (ft.)	TC (corr.cps)	K (corr.cps)	U (corr.cps)	Th (corr.cps)	Avg. Alt. (m)
50100	14.97	774.75	58.26	11.87	25.18	4.56
50150	58.55	712.08	51.29	11.96	21.15	17.85
50200	102.37	677.14	46.50	10.97	21.84	31.21
50250	152.36	647.86	45.12	10.48	20.51	46.45
50300	196.36	555.37	38.53	9.56	16.81	59.87
50350	246.19	534.70	33.91	9.55	16.37	75.06
50400	299.67	488.48	32.28	9.13	14.09	91.36
50450	348.59	449.63	26.59	8.95	13.08	106.28
50500	394.59	418.58	25.83	8.93	11.40	120.30

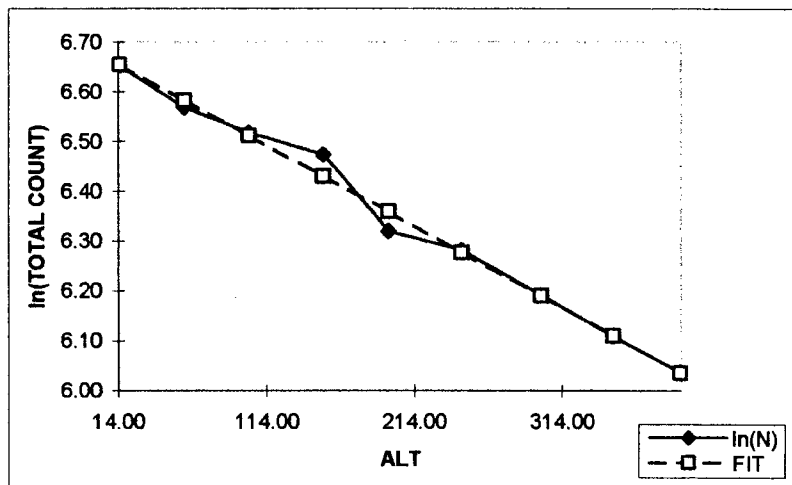
##### RESULTS OF LSQ TO $\ln(N) = \text{ALT} \cdot \mu + \ln(N_0)$ RELATION:

TC	$\mu_{TC} =$	-0.001628	$\ln(N_0)_{TC}$	6.67819
K	$\mu_K =$	-0.002168	$\ln(N_0)_K$	4.084944
U	$\mu_U =$	-0.000972	$\ln(N_0)_U$	2.501068
Th	$\mu_{Th} =$	-0.001987	$\ln(N_0)_{Th}$	3.250358

##### GRAPHICAL DISPLAYS OF MEASURED AND FITTED DATA :

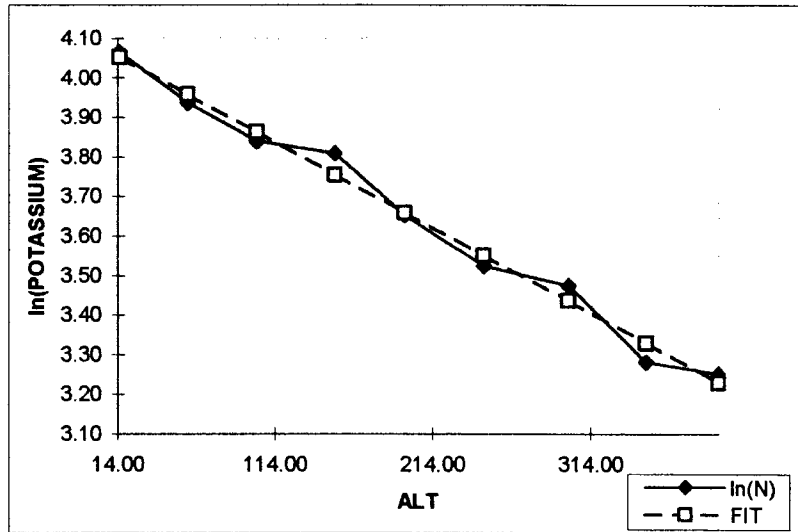
##### TOTAL COUNT:

ALT	$\ln(N)$	FIT
14.97	6.65	6.65
58.55	6.57	6.58
102.37	6.52	6.51
152.36	6.47	6.43
196.36	6.32	6.36
246.19	6.28	6.28
299.67	6.19	6.19
348.59	6.11	6.11
394.59	6.04	6.04



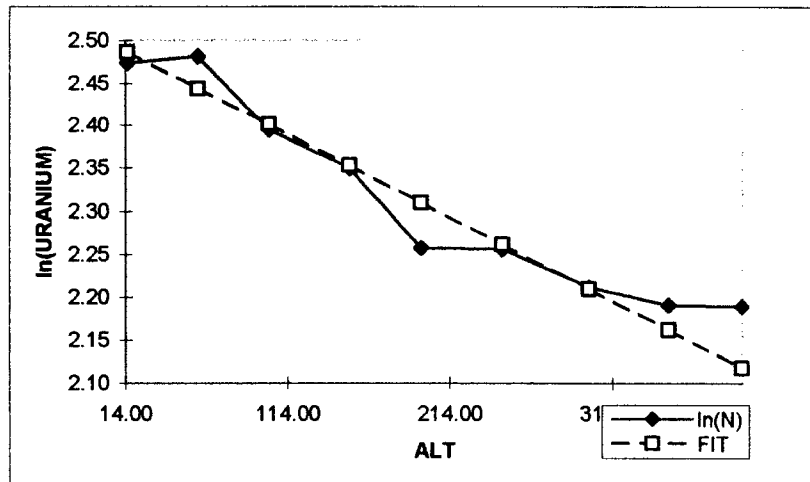
**POTASSIUM:**

ALT	ln(N)	FIT
14.97	4.06	4.05
58.55	3.94	3.96
102.37	3.84	3.86
152.36	3.81	3.75
196.36	3.65	3.66
246.19	3.52	3.55
299.67	3.47	3.44
348.59	3.28	3.33
394.59	3.25	3.23



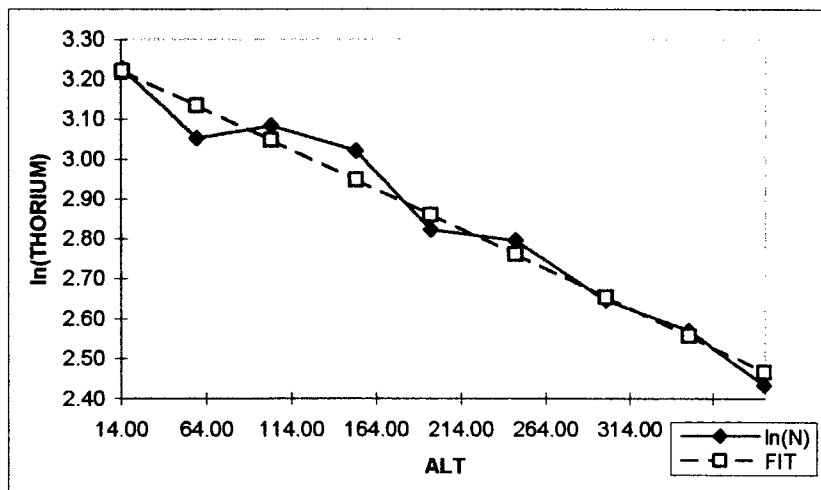
**URANIUM:**

ALT	ln(N)	FIT
14.97	2.47	2.49
58.55	2.48	2.44
102.37	2.40	2.40
152.36	2.35	2.35
196.36	2.26	2.31
246.19	2.26	2.26
299.67	2.21	2.21
348.59	2.19	2.16
394.59	2.19	2.12



**THORIUM:**

ALT	ln(N)	FIT
14.97	3.23	3.22
58.55	3.05	3.13
102.37	3.08	3.05
152.36	3.02	2.95
196.36	2.82	2.86
246.19	2.80	2.76
299.67	2.65	2.65
348.59	2.57	2.56
394.59	2.43	2.47



**APPENDIX F**

**ARCHIVE DESCRIPTION**

## APPENDIX F

### ARCHIVE DESCRIPTION

Reference: CCD01543  
Disc 1 of 1  
Volume Label: "2058"  
Archive Date: 2001-SEP-04

-----  
This archive contains FINAL DATA ARCHIVES of a DIGHEM airborne geophysical survey conducted by FUGRO AIRBORNE SURVEYS CORP. on behalf of MANSON CREEK RESOURCES LTD. for BLOCKS TANNER in YUKON TERRITORY during JULY, 2001

Job # 2058

-----  
This archive comprises 46 files contained in 3 directories

\*\*\*\*\* Disc 1 of 1 \*\*\*\*\*

#### GRIDS\

Grids in Geosoft binary (2-byte) format

MAG_*.GRD	- Total Magnetic Field
CVG_*.GRD	- Magnetic Vertical Gradient
RES900_*.GRD	- Apparent Resistivity 900 Hz coplanar
RES7200_*.GRD	- Apparent Resistivity 7200 Hz coplanar
RES56K_*.GRD	- Apparent Resistivity 56 kHz coplanar
TC_*.GRD	- Total Count
K_*.GRD	- Potassium
U_*.GRD	- Uranium
TH_*.GRD	- Thorium

For the Tanner block, \* is C

#### LINEDATA\

2058C.XYZ	- ASCII line data archive in Geosoft XYZ format for the Tanner block
2058.TXT	- ASCII text description file for the XYZ data archive
AN2058C.XYZ	- ASCII EM anomaly listing in Geosoft format for the Tanner block



Resitivity is calculated using a proprietary pseudo-layer half-space algorithm.

---

The coordinate system for all grids and XYZ files is projected as follows

Datum	NAD27
Spheroid	Clarke 1866
Projection	UTM Zone 8N
Central meridian	-135
False easting	500000
False northing	0
Scale factor	0.9996
Northern parallel	N/A
Base parallel	N/A
WGS84 to local conversion method	Molodensky
Delta X shift	+7
Delta Y shift	-139
Delta Z shift	-181

---

If you have any problems with this archive please contact

Manager, Interpretation and Processing  
FUGRO AIRBORNE SURVEYS CORP.  
2270 Argentia Road, Unit 2  
Mississauga, Ontario  
Canada L5N 6A6  
Tel (905) 812-0212  
Fax (905) 812-1504  
E-mail [toronto@fugroairborne.com](mailto:toronto@fugroairborne.com)